Bounds on Autonomous Quantum Error Correction

Oles Shtanko[*1], Yu-Jie Liu[*2,3], Simon Lieu [†4,5], Alexey V. Gorshkov[4,5], and Victor V. Albert[5]

[1]IBM Quantum, IBM Research – Almaden, San Jose, CA, USA
[2]Technical University of Munich, TUM School of Natural Sciences, Physics Department, 85748 Garching, Germany
[3]Munich Center for Quantum Science and Technology (MCQST), Munich, Germany
[4]Joint Quantum Institute, NIST/University of Maryland, College Park, MD, USA
[5]Joint Center for Quantum Information and Computer Science, NIST/University of Maryland, College Park, MD, USA

Abstract

Autonomous quantum memories are a way to passively protect quantum information using engineered dissipation that creates an "always-on" decoder. We analyze Markovian autonomous decoders that can be implemented with a wide range of qubit and bosonic error-correcting codes, and derive several upper bounds and a lower bound on the logical error rate in terms of correction and noise rates. For many-body quantum codes, we show that, to achieve error suppression comparable to active error correction, autonomous decoders generally require correction rates that grow with code size. For codes with a threshold, we show that it is possible to achieve faster-than-polynomial decay of the logical error rate with code size by using superlogarithmic scaling of the correction rate. We illustrate our results with several examples. One example is an exactly solvable global dissipative toric code model that can achieve an effective logical error rate that decreases exponentially with the linear lattice size, provided that the recovery rate grows proportionally with the linear lattice size.

One of the biggest challenges in quantum computing is the problem of noise. Any realistic qubit architecture is prone to dissipation due to interactions with the environment, leading to errors and subsequent loss of quantum information. Traditional error correction strategies have focused on manual periodic error diagnosis and correction [1, 2]. In recent years, however, there has been a surge in autonomous "hardware" methods designed to compensate for noise using engineered dissipation [3–7]. Several dissipative quantum memories have been successfully implemented experimentally, in particular using various bosonic codes[1] [9–15], but they have not been fully exploited for error correction in real many-body systems consisting of several qubits or qudits.

---

[*]These authors contributed equally.

[†]This work was done prior to joining AWS.

[1]The name of each code, when introduced for the first time in the manuscript, will contain a hyperlink to the code's corresponding webpage in the Error Correction Zoo [8].

A topic closely related to dissipatively stabilized quantum memories is self-correction [16], a process in which the propagation of errors is naturally limited without performing active error correction. An example of self-correction in the classical world is the storage of information in magnetic hard drives. Here, classical information is encoded in a ferromagnet by its collective spin magnetization, and errors resulting from spontaneous individual spin flips become energetically unfavorable and are therefore eliminated by a local thermalization process. This mechanism ensures a memory lifetime that scales exponentially with system size [17, 18].

The principle of classical self-correction can be extended to quantum systems, such as those stabilized by frustration-free Hamiltonians [2]. For example, the four-dimensional toric code [19] demonstrates a finite-temperature topological order that naturally protects quantum information [20–22]. Unfortunately, several no-go results preclude local frustration-free Hamiltonians from achieving self-correction with a constant error rate in two dimensions [23–26] and for some three-dimensional models [27–29]. Such studies are also hampered by broad challenges associated with quantum complexity [30–33].

The use of dissipative processes to aid or induce self-correction in quantum systems continues to be actively studied. In some cases, it is possible to show numerically that lower-dimensional systems can still offer quantum memory times that grow with system size [34–39]. However, there is currently no unified approach that allows general conclusions to be drawn about memory performance, and there are no universal bounds on the aid that a dissipative process can provide.

In this work we derive a general non-perturbative bound (see Theorem 1), valid for a wide class of autonomous quantum memories and restricted by only a few intuitive assumptions. This bound expresses the logical error rate of a dissipative memory in terms of the noise-to-recovery ratio — the ratio between the benevolent recovery dissipation rates and the strength of any malevolent noise. The core idea is to use the resummation of Dyson's perturbative expansion, which allows one to derive the logical error in the late-time limit. We show that, as soon as the noise-to-recovery ratio is less than a critical value, autonomous memory can achieve lifetimes that grow exponentially with the inverse noise rate. At the same time, this general bound promises an exponentially small logical error rate only if the recovery rate grows with system size.

To understand better the results of Theorem 1, we specialize our analysis to a subclass of dissipative memories that we call *global decoders*. This specific model represents an oversimplified recovery process that takes any error state *directly* into the codespace. Although this model is technically different from many dissipative memories that use the gradual relaxation of error states into the codespace, it serves as an exactly solvable example of decoding dynamics. As we will show below, it also saturates the logical error rate bound established in Theorem 1.

Our global decoder model can be seen as an autonomous version of active error correction with the assumption that rounds of error correction essentially "take zero time" (cf. [40]). We compress syndrome extraction, any classical post-processing involved in decoding, and the corresponding recovery operation into a pre-compiled procedure—in the form of a series of *jump operators*—that is implemented instantaneously and autonomously. As such, the model can be seen as an idealized form of autonomous correction for which local syndrome measurements, efficient decoders, and recoveries are implemented instantaneously at random

Type of the results on $\epsilon(t)$	Section	Noise type	Comments
Upper bound (Thm. 1)	2	Generic	Applicable to generic noise
Asymptotics at late time	3.1	Poissonian	Valid only for late times
Upper bound (Thm. 2)	3.2	Poissonian	Tight for intermediate times
Upper bound (Thm. 3)	3.2	Pauli	Improved Thm. 2 for Pauli noise
Upper bound (Thm. 4)	3.3	Poissonian	Tight for short times
Lower bound	4	Pauli	Restricted to stabilizer codes

Table 1: Summary of the results. Here $\epsilon(t)$ measures the logical error probability at time t as defined in Section 1. The notion of Poissonian noise is discussed in Section 3.

times.

Our global decoder assumption, while seemingly unphysical, demonstrates that autonomous memories, including those utilizing seemingly limitless resources, do not guarantee performance comparable to active error correction. We find that the assumption of immediate system-wide corrections does not automatically yield memory times that scale exponentially, or even polynomially, with system size. For multi-qubit systems undergoing Pauli noise, we show that memory lifetime scales exponentially only with the ratio of two values: the code distance multiplied by recovery process rate and the *total* error rate (i.e. sum of error rates for each physical qubit)—see Theorem 2 and the discussion around it. Thus, even if the code distance grows linearly with system size (as in the case of asymptotically good quantum low-density parity-check (QLDPC) codes [41–43]), the correction rate must grow with system size to yield system-size growing memory lifetime. By providing a lower bound derived for a subclass of models with Pauli noise, we also show that this scaling cannot be improved.

The conclusion implied by the bounds described above is that it is impossible to obtain a global decoder with either exponential or polynomial lifetime using our seemingly powerful engineered dissipation with a constant recovery rate. This result illustrates that the details of the recovery process matter, and the simple fact that it has dissipative gap—i.e. it gets the system into the codespace in finite time—alone is not enough for a scalable dissipative memory.

It is noteworthy that the global decoder model combined with Pauli noise is an example of a *Poissonian* process. Such Lindbladian dynamics can be represented as a sum of independently sampled stochastic trajectories, including error and recovery quantum channels. This representation allows us to bound the performance of the global decoder by counting the trajectories that lead to a logical error. This representation also provides a simple intuitive picture of the complex noisy dynamics. This idea may also be useful to obtain bounds on the relaxation time for perturbed local Lindbladians [22], which would otherwise typically require detailed balance, among other assumptions [20, 44–46].

The remainder of the manuscript is organized as follows. In Section 1, we introduce the model of a dissipative memory and, in particular, the global decoder. Next, in Section 2, we provide a logical error bound for general dissipative memories that satisfy a few minimal assumptions. To improve this result, in Section 3, we introduce the Poisson error model, which,

acting in the presence of the global decoder model, has a better bound on the logical error probability obtained by counting the stochastic trajectories. In particular, in Section 3.1, we derive the asymptotic late-time behavior of the process using this stochastic trajectory representation. In Sections 3.2 and 3.3, we generalize this result by giving upper bounds on the performance of the global decoder. To justify the tightness of this result, in Section 4, we derive a lower bound on the logical error probability for a special case of models with Pauli noise. Finally, in Section 5, we present several examples and study them numerically. The last Section 6, contains a discussion and outlook. The summary of the results can also be found in Table 1.

1 Model

Our model of an autonomous quantum memory consists of three ingredients: a noisy quantum system, a codespace, and a recovery map.

Noisy system. We consider a noisy quantum system with Markovian noise [47] and accessible Hilbert space H of dimension $2D$. The evolution of the system, in the absence of external control, is characterized by the Lindblad master equation [48, 49]

$$\frac{d}{dt}\rho = \Delta \mathcal{L}_E \rho, \tag{1}$$

where ρ is the density matrix of the system, Δ is the noise rate, and $\mathcal{L}_E$ is the *error Lindbladian* that takes the form

$$\mathcal{L}_E = \sum_{\mu=1}^{N} \lambda_\mu \Big(E_\mu \rho E_\mu^\dagger - \frac{1}{2}\{E_\mu^\dagger E_\mu, \rho\}\Big). \tag{2}$$

Here, the N error operators $\{E_\mu\}_{\mu=1}^N$ have spectral norm $\|E_\mu\| = 1$, and $\lambda_\mu > 0$ are real weights satisfying $\sum_\mu \lambda_\mu = N$.

We choose error operators to be sufficiently general to encompass both noise models in many-body systems, for which the Hilbert space H has a tensor-product structure, as well as in single bosonic modes, for which H is embedded in a single countably infinite space. As such, the error jump operators E_μ should be interpreted as the generators of error combinations, or strings, that constitute our model's error set. The accumulated error operators are $K_{\boldsymbol{\mu}} := K_{\mu_1} \ldots K_{\mu_k}$ labeled by all possible error sequences $\boldsymbol{\mu} = (\mu_1, \ldots, \mu_k)$, where $k \geq 1$, and the elementary errors in the sequence are

$$K_\mu \in \{E_1, \ldots, E_N, E_1^\dagger E_1, \ldots, E_N^\dagger E_N\} . \tag{3}$$

The set of elementary errors includes quadratic combinations of jump operators, such as $E_\mu^\dagger E_\mu$, manifested in the last term of the Lindblad equation. When we decompose the Lindblad evolution into many stochastic trajectories, this term of the Lindblad equation characterizes the error accumulated between the error jumps. It is important to note, however, that these quadratic errors loose their relevance for unitary error operators E_μ. In these situations, quadratic errors become trivial and should be ignored.

4
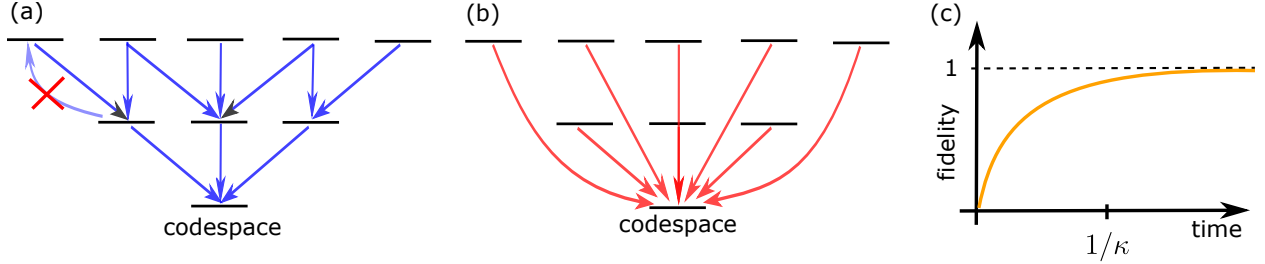
Figure 1: **Autonomous error correction.** The horizontal lines in (a) and (b) represent different error subspaces in the Hilbert space H, including the codespace C. (a) General model of autonomous error correction: the correction process causes transitions between error states, lowering the effective error weight until the system reaches the codespace. (b) Global decoder: the recovery process causes transitions directly into the code space. (c) Starting with an arbitrary initial state, the fidelity (i.e. the probability of being in the codespace) in the absence of error processes approaches one with rate κ, for both general and global decoders.

In the case of qubit codes, the error jump operators E_μ are often Pauli operators acting on a single or a few qubits, while the $K_{\boldsymbol{\mu}}$ are tensor products of such operators. In this scenario, many error sequences are equivalent since, for example, two Pauli errors cancel each other out, $E_\mu^2 = I$. Therefore, we count only unique errors as part of the full set of $K_{\boldsymbol{\mu}}$. In another example of a bosonic mode undergoing photon loss, the only jump operator E_μ is the bosonic annihilation operator, and $K_{\boldsymbol{\mu}}$ are powers of that operator and its adjoint, the creation operator. In all cases, the length of $\boldsymbol{\mu}$, denoted as $|\boldsymbol{\mu}|$, provides an upper bound on the number of resulting accumulated errors and quantifies their potential severity. We will sometimes refer to $|\boldsymbol{\mu}|$ as the weight of the error.

Codespace. We consider a single qubit of logical quantum information encoded in the codespace C $\in$ H. We further assume that C is a quantum code with *error radius* ℓ, defined as the largest number for which all errors of weight ℓ and below are correctable. In particular, a code with error radius ℓ satisfies the Knill-Laflamme condition [50]

$$PK_{\boldsymbol{\mu}}^\dagger K_{\boldsymbol{\nu}} P = C_{\boldsymbol{\mu}\boldsymbol{\nu}} P \qquad \forall \boldsymbol{\mu}, \boldsymbol{\nu} \quad \text{such that} \quad |\boldsymbol{\mu}|, |\boldsymbol{\nu}| \leq \ell \,, \tag{4}$$

where $C_{\boldsymbol{\mu}\boldsymbol{\nu}}$ are constants, and P is the projector on the codespace. At the same time, there exist one or more errors of weight $\ell+1$ such that, when added to the above set of correctable errors, they violate Eq. (4). For example, qubit codes undergoing Pauli noise with distance d have error radius $\ell = \lfloor (d-1)/2 \rfloor$ with respect to local Pauli noise. On the other hand, bosonic rotation codes [51] undergoing photon loss and being able to detect S photon losses have an error radius of $\lfloor S/2 \rfloor$ with respect to loss errors.

Recovery process. We consider the autonomous correction process with evolution equation

$$\frac{d}{dt}\rho = \mathcal{L}_R \rho, \tag{5}$$

where $\mathcal{L}_R$ is the Lindbladian generator of the recovery dynamics. An initial state $\rho(0) = \rho_0$ evolving under this Lindbladian to time t can be written as

$$\rho(t) = e^{-\kappa t}\mathcal{K}_t(\rho_0) + (1 - e^{-\kappa t})\mathcal{R}(\rho_0), \tag{6}$$

5

where $\mathcal{R} = \mathcal{R}^2$ is a quantum channel recovering information into the codespace (more generally, the right kernel of $\mathcal{L}_\mathcal{R}$). The remaining term $e^{-\kappa t}(\mathcal{K}_t - \mathcal{R})$ acts on eigenspaces of the Lindbladian corresponding to eigenvalues with nonzero real parts [52] [53, Eq. (1.35)]. We have expressed this term using $\mathcal{K}_t$ (where $\mathcal{K}_0 = \mathcal{I}$ is the identity), which can be thought of as a *partial recovery map* that can be designed to reduce error weight in local regions without fully recovering in code space. We have explicitly written the partial recovery map in terms of the *dissipative gap* κ—the nonzero eigenvalue of $\mathcal{L}_\mathcal{R}$ with the smallest real part—such that it has a spectral radius bounded by one.

For this work, we specialize to a class of maps that can be described as decoders by making three assumptions. Our first and mildest assumption is that $\mathcal{K}_t$ is diagonalizable, meaning that its spectral norm is bounded above by one. Second, we assume that the dynamics in Eq. (5) represent a valid recovery process; this means that the dissipative gap κ is nonzero and the recovery map $\mathcal{R}$ corresponding to $\mathcal{L}_R$ corrects errors up to the error radius,

$$\mathcal{R}(K_{\boldsymbol{\mu}} \rho_0 K_{\boldsymbol{\nu}}^\dagger) \propto \rho_0 \qquad \forall \quad |\boldsymbol{\mu}|, |\boldsymbol{\nu}| \leq \ell. \tag{7a}$$

In other words, any state, after the application of a correctable error, returns to the codespace without a logical error having occurred. We discuss how to construct such recovery operators in Appendix A.

Third, we assume that any intermediate-time recoveries *do not increase* the weight of an error state (see Fig. 1a), i.e. for all $t \geq 0$,

$$\exp(\mathcal{L}_R t)(K_{\boldsymbol{\mu}} \rho_0 K_{\boldsymbol{\nu}}^\dagger) = \sum_{\boldsymbol{\mu}' \boldsymbol{\nu}'} a_{\boldsymbol{\mu\nu},\boldsymbol{\mu}'\boldsymbol{\nu}'}(t) K_{\boldsymbol{\mu}'} \rho_0 K_{\boldsymbol{\nu}'}^\dagger, \tag{7b}$$

where $a_{\boldsymbol{\mu\nu},\boldsymbol{\mu}'\boldsymbol{\nu}'}(t) = 0$ if $|\boldsymbol{\mu}'| > |\boldsymbol{\mu}|$ or $|\boldsymbol{\nu}'| > |\boldsymbol{\nu}|$. This idealization rules out well-performing decoders that can increase error weight even for negligible subsets of error configurations. However, it allows us to derive our main result in Theorem 1.

Most of our results concern the *global decoder model*, which is a special case of the model in Eq. (6) with assumptions in Eq. (7) where we additionally remove any partial recovery, i.e. we assume $\mathcal{K}_t \equiv \mathcal{I}$. In this case, the Lindladian for the recovery process is given by

$$\mathcal{L}_R = \kappa\big(\mathcal{R}(\rho) - \rho\big), \qquad \rho(t) = e^{-\kappa t} \rho_0 + (1 - e^{-\kappa t})\mathcal{R}(\rho_0). \tag{8}$$

In this model, the recovery dynamics return error states directly to the codespace (see Fig. 1b). The recovery $\mathcal{R}$ may act non-locally in order to recover information into the codespace in one step. The definition of the dissipative gap remains the same for both general and such global decoders (see Fig. 1c).

Logical errors and critical error rate. The combination of the recovery process and the error process results in a dynamical equation that describes the autonomous quantum memory:

$$\frac{d}{dt}\rho = \mathcal{L}(\rho) := \mathcal{L}_R(\rho) + \Delta \mathcal{L}_E(\rho). \tag{9}$$

Our goal is to explore the performance of such a quantum memory. In particular, we aim to find a regime where, in the presence of noise ($\Delta > 0$), the probability of a logical error

6

after recovery for a family of codes with increasing ℓ vanishes polynomially or exponentially in the limit $\ell \to \infty$.

As a measure to quantify logical errors, we consider the trace distance as a function of time between two initially orthogonal pure states in the codespace and define the following error measure:

$$\delta(t) := 1 - \min_{\rho_0} T(\exp(\mathcal{L}t)\rho_0, \exp(\mathcal{L}t)\rho_0^{\perp}), \quad \rho_0 = |\psi_0\rangle\langle\psi_0|, \quad |\psi_0\rangle \in \mathsf{C}, \tag{10}$$

where $T(\rho, \sigma)$ is the trace distance between states ρ and σ. This error measure vanishes if and only if there exists a recovery map that always returns the logical qubit to its initial, error-free configuration. However, such a map may be complex and a priori unknown.

As an alternative, we define a simpler logical error measure that quantifies our ability to recover information using the recovery map $\mathcal{R}$ based on the fidelity of recovery starting from a pure initial state:

$$\epsilon(t) := 1 - \min_{\rho_0} \text{Tr}\left[\rho_0 \mathcal{R} \exp(\mathcal{L}t)\rho_0\right], \quad \rho_0 = |\psi_0\rangle\langle\psi_0|, \quad |\psi_0\rangle \in \mathsf{C}, \tag{11}$$

where the minimum, as in Eq. (10), is taken over pure states in the codespace.

For a single logical qubit, the two error measures $\delta(t)$ and $\epsilon(t)$ are related by (see Appendix A)

$$\delta(t) \leq 2\epsilon(t) . \tag{12}$$

We will focus below on the measure $\epsilon(t)$ in Eq. (11). However, some results also apply to $\delta(t)$ (see Theorems 1 and 4 below).

2 General bound and critical rate

In this section, we present a result that shows that autonomous memories always exhibit exponential memory lifetimes for sufficiently small noise rate. To do this, we must first introduce a parameter that quantifies the strength of the noise. We first introduce a space of errors K spanned on the error states $|\psi_{w\boldsymbol{\mu}}\rangle \propto K_{\boldsymbol{\mu}}|w\rangle$, where $w \in \{0, 1\}$ and $K_{\boldsymbol{\mu}}$ are errors of weight smaller that ℓ that stisfy the condition in Eq. (4). Then we can introduce $\|\mathcal{L}_E\|_{\mathsf{K}}$ as the spectral norm of the superoperator $\mathcal{L}_E$ over the subspace $\mathsf{K} \subset \mathsf{H}$, i.e. $\|\mathcal{L}_E\|_{\mathsf{K}} := \max_{O\in\text{End}(\mathsf{K})} \|\mathcal{L}_E(O)\|_2/\|O\|_2$, where $\text{End}(\mathsf{K})$ is the space of endomorphisms in K and $\|\cdot\|_2$ is the Euclidean norm. By definition, for finite systems this norm is bounded by the spectral norm, i.e. $\|\mathcal{L}_E\|_{\mathsf{K}} \leq \|\mathcal{L}_E\|_{\mathsf{H}} \equiv \|\mathcal{L}_E\|$.

Then we can write our first result as the following theorem:

Theorem 1. *For an arbitrary error model and a diagonalizable recovery map that satisfies the assumptions in Eq. (7), the error rate is bounded by*

$$\epsilon(t), \delta(t) \leq \left(\frac{\Delta\|\mathcal{L}_E\|_{\mathsf{K}}}{\kappa}\right)^{\ell+1} F_\ell(\kappa t) \leq \left(\frac{\Delta\|\mathcal{L}_E\|_{\mathsf{K}}}{\kappa}\right)^{\ell+1} \kappa t \equiv \eta^{\ell+1}\kappa t , \tag{13}$$

where $F_\ell(z) = zg(\ell, z) - \ell g(\ell + 1, z) \leq z$, and $g(\ell, z)$ is the regularized lower incomplete Gamma function [54].
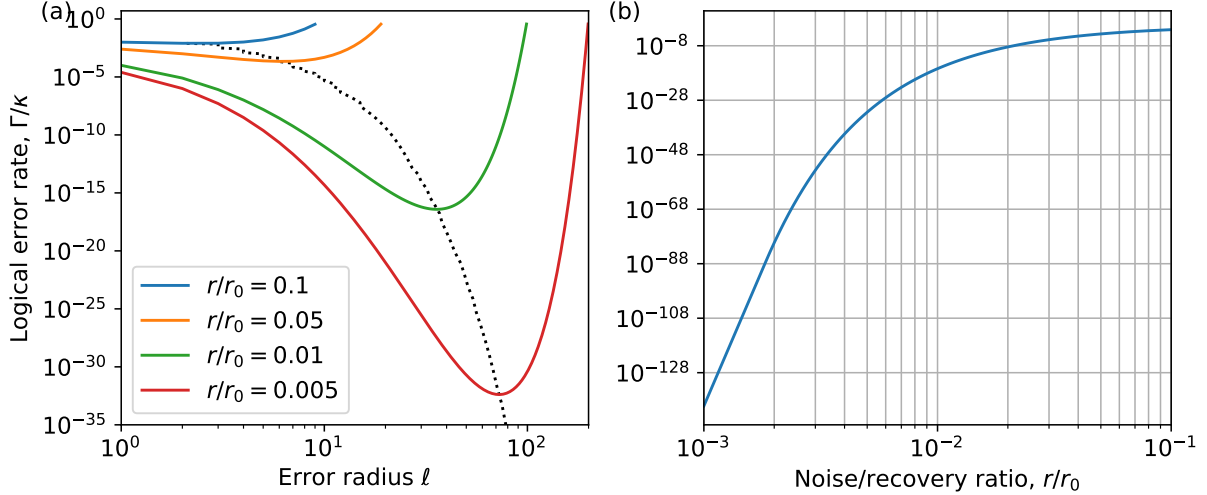
Figure 2: **Logical rate for generic qubit-based models.** (a) The logical rate as a function of the error radius for different values of the noise-to-recovery ratio r. The function has a minimum for $\ell_{\min} = O(r_0/r)$, the positions of the minima are shown as the dotted black curve. (b) The minimum logical error rate ratio as a function of the noise-to-recovery ratio, see Eq. (14).

To prove this result, we use Dyson's perturbative expansion of the evolution superoperator with Δ as a small parameter. We show that the first ℓ perturbative terms in the series vanish, and use a re-summation of the remaining terms to obtain a non-perturbative expression. The proof can be found in Appendix B. Note that this result holds not only for finite-dimensional systems, but also for certain (infinite-dimensional) bosonic systems where K is a finite subspace.

For small values of $\kappa t \ll 1$, with all other parameters fixed, the error bound scales as $O((\Delta \|\mathcal{L}_E\|_\mathsf{K} t)^{\ell+1})$. This reflects the fact that, in this limit, the error is described by perturbation theory and the lowest non-vanishing terms are of order $\ell + 1$. In contrast, in the non-perturbative regime $\kappa t \gg 1$, the logical error bound grows linearly and its rate is proportional to $\eta^{\ell+1}$, where $\eta = \Delta \|\mathcal{L}_E\|_\mathsf{K}/\kappa$. Therefore, this rate is exponentially suppressed in ℓ if the noise is small enough that $\eta < 1$.

Let us analyze this suppression for certain multi-qubit codes for constant recovery rate κ. In multi-qubit systems, the Lindblad operators have norm $\|\mathcal{L}_E\|_\mathsf{K} \leq \|\mathcal{L}_E\| = cn$, where the dimensionless multiplication factor c reflects the rate of local error processes. One can also find QLDPC codes whose radius is proportional to the number of qubits, such that $\ell \geq \alpha n$ for some $\alpha < 1$. As a result, the logical error rate is $\Gamma := \delta(t)/t \leq (\ell r/r_0)^{\ell+1}\kappa$, where $r = \Delta/\kappa$ is a renormalized noise to recovery ratio and $r_0 = \alpha/c$. Unlike in active error correction, the logical error rate bound does not become arbitrarily small for ever-increasing ℓ. In fact, for small $r \ll 1$, the bound has its minimum at $\ell \simeq r_0/er$, where e is the base of the natural logarithm. This dependency is shown in Fig. 2(a). The minimum logical error rate bound is

$$\Gamma_{\min} = O\left(\kappa e^{-r_0/r}\right), \qquad r = \Delta/\kappa. \tag{14}$$

8

This is the minimum error rate bound for fixed κ. Therefore, we show that, for constant κ, there exists a universal upper bound on the error rate that is sufficiently smaller than the original error rate Δ once $r < r_0$. In this regime, a small improvement in the error rate Δ yields, at least, an exponential improvement in the logical error rate bound, see Fig. 2(b). This constitutes a universal "soft threshold" result applicable to arbitrary autonomous error-correcting codes based on QLDPC codes.

Of course, we know that this bound is not tight: for some autonomous codes we can have arbitrarily small errors for some Δ/κ below the threshold [20–22]. However, our result suggests that, in general, to get such unbounded error reduction, we must have $\kappa \sim \|\mathcal{L}_E\|$, i.e., growing with system size. In fact, by considering a particular example below in Section 4, we show that this scaling condition cannot be relaxed in general.

3 Global decoders and a Poissonian error model

In this section, we derive tighter bounds than the generic-decoders bound in Eq. (13) by focusing on global decoders in Eq. (8) and specializing to unitary error jump operators (including Pauli noise). Such bounds allow for a better grasp of the capabilities of a recovery rate κ that is sublinear in the number of qubits.

Let us consider a simplification of the quantum dynamics, given that error operators in Eq. (2) that are unitary, $E_\mu^\dagger E_\mu = I$, where I is the identity matrix. We refer to this dynamics as *Poissonian* as it maps directly to a Poissonian point process [55]. While this restriction still covers generic Pauli noise for qubit, modular-qudit [56], and Galois-qudit codes [57,58], it does not include processes such as photon loss or additive Gaussian white noise applicable to bosonic codes.

Assuming Poissonian errors, we can rewrite the Lindblad equation in Eq. (9) as

$$
\frac{d}{dt}\rho = \mathcal{L}(\rho) = \gamma \sum_{\mu=0}^{N} p_\mu\big(\mathcal{E}_\mu(\rho) - \rho\big), \qquad \text{where} \qquad \mathcal{E}_\mu(\rho) = \begin{cases} \mathcal{R}(\rho) & \mu = 0 \\ E_\mu \rho E_\mu^\dagger & \mu > 0 \end{cases}, \tag{15}
$$

where $\gamma = \kappa + N\Delta$, $p_0 = \kappa/\gamma$, and $p_{\mu>0} = \lambda_\mu \Delta/\gamma$. Notably, parameters p_μ are positive, satisfy the normalization condition $\sum_\mu p_\mu = 1$, and can therefore be treated as probabilities.

The formal solution of Eq. (15) is obtained from the exponentiation of $\mathcal{L}$, which takes the form of a sum of multiple stochastic trajectories:

$$
\exp(\mathcal{L}t) = e^{-\gamma t} \exp\left(\gamma t \sum_{\mu=0}^{N} p_\mu \mathcal{E}_\mu \right) = \sum_{\boldsymbol{\mu} \in F} p(\boldsymbol{\mu}, t)\mathcal{E}_{\boldsymbol{\mu}}, \tag{16a}
$$

where the set F includes trajectories $\boldsymbol{\mu}$ of any length, including consequent errors and recoveries, and $\mathcal{E}_{\boldsymbol{\mu}} = \mathcal{E}_{\mu_k} \circ \cdots \circ \mathcal{E}_{\mu_1}$, where $\circ$ denotes the composition of superoperators (we omit it below). The probability of a trajectory of error weight $|\boldsymbol{\mu}| = k$ occurring at time t has the form

$$
p(\boldsymbol{\mu}, t) = \frac{1}{k!}(\gamma t)^k e^{-\gamma t} p_{\mu_1} \ldots p_{\mu_k}, \tag{17}
$$

where probabilities p_μ are defined below Eq. (15). It is easy to confirm that, for a given t, the probabilities $p(\boldsymbol{\mu}, t)$ for any time t sum to one. As a result, we can interpret the dynamics as

a homogeneous Poisson point process, in which error and recovery events occur at random times following a Poisson distribution with average spacing γ^{-1}.

3.1 Asymptotic logical error estimate for Poissonian models

Using the Poisson picture, we can derive a bound on the logical error rate by counting how many trajectories do not contribute to the logical error. First, we specify such trajectories using the following definition.

Definition 1. *We say that a trajectory $\boldsymbol{\mu} = (\mu_1, \ldots, \mu_q)$ of weight q is faithful if it contains no error subsequence of length $m > \ell$, i.e. a subsequence $\{\mu_k, \ldots, \mu_{k+m-1}\}$ for $1 \leq k \leq q - m + 1$ such that all $\mu_{k+i} > 0$.*

In other words, faithful trajectories contain no uninterrupted error sequences of length greater than ℓ. The total probability of faithful trajectories provides a lower bound on the probability that no logical error occurs (see the lemma below).

In passing, it is important to note that in general not all trajectories that are not faithful contribute to the logical error. For example, a sequence of more than ℓ Pauli errors does not contribute to a logical error if it can be reduced to a weight less than ℓ by canceling identical errors. However, since we are only aiming for an upper bound on the logical error, one can exclude these trajectories from consideration and still keep the bound valid.

Let the full set of faithful trajectories be denoted by G. Then the logical error probability is bounded as:

Lemma 1. *For a Poissonian error process in Eq. (16), the error in Eq. (11) satisfies*

$$\epsilon(t) \leq p(t) := \sum_{\boldsymbol{\mu} \in F \setminus G} p(\boldsymbol{\mu}, t) \ , \tag{18}$$

where $F \setminus G$ stands for trajectories that are not faithful.

The proof of this lemma can be found in Appendix C. This lemma allows us to derive the upper bound on the logical error Eq. (18) by counting faithful trajectories. We exploit the fact that errors and recoveries are independent stochastic processes. Then, for any trajectory of time t, the probability of m recoveries is equal to $R(m, \kappa t)$, where $R(m, x) := (\kappa t)^m e^{-x}/m!$ (see Eq. (17)). The total probability of getting an non-faithful trajectory is given then by

$$p(t) = 1 - \sum_{m=0}^{\infty} R(m, \kappa t) \int_0^t dt_1 \pi(t_1|t) s(t_1) \int_0^{t-t_1} dt_2 \pi(t_2|t - t_1) s(t_2)$$
$$\cdots \int_0^{t-t_1 \cdots -t_{m-1}} dt_m \pi(t_m|t - t_1 \cdots - t_{m-1}) s(t_m) s(t - t_1 \cdots - t_m), \tag{19}$$

where $\pi(t_i|t)$ is the probability that the time of the first recovery event in a random sequence is t_i conditioned on the total evolution time t, and $s(t_i)$ is the probability that the error process during the interval $[0, t_i]$ does not result in an error weight larger than ℓ,

$$\pi(t_i|t) = \frac{\kappa \exp(-\kappa t_i)}{1 - \exp(-\kappa t)}, \qquad s(t_i) = \sum_{k=0}^{\ell} R(k, N\Delta t_i). \tag{20}$$

In the asymptotic limit $\kappa t \gg 1$, we can provide a (non-rigorous) estimate for the probability in Eq. (19) by extending the upper limits of integration limits and conditioned evolution times to infinity, as well as ignoring the contribution of the last term, which leads us to

$$p(t) \approx 1 - \sum_{m=0}^{\infty} R(m,t) \left(\int_0^{\infty} d\tau \pi(\tau|\infty)s(\tau) \right)^m = 1 - \exp(-\Delta_{\mathrm{eff}}t), \tag{21}$$

where the effective logical error rate is

$$\Delta_{\mathrm{eff}} = \frac{\kappa}{\left(1 + \frac{\kappa}{N\Delta} \right)^{\ell+1}}. \tag{22}$$

Let us examine the above expression from the standpoint of memory lifetime for multiqubit codes. Assuming that each qubit is subject to at least one type of error, the number of elementary error processes grows with the number of qubits n, i.e. $N = \Theta(n)$.[2] Using the asymptotic behavior in Eq. (22), we then get the scaling (for a constant Δ):

$$\Delta_{\mathrm{eff}} = \begin{cases} \kappa \exp(-\Theta(\kappa\ell/n\Delta)) & \kappa = o(n), \\ \kappa \left(\frac{\kappa}{n\Delta} \right)^{-\Theta(\ell)} & \kappa = \Omega(n), \end{cases} \tag{23}$$

where all parameters, i.e. $\kappa = \kappa(n)$, $\ell = \ell(n)$, must be treated as functions of the number of qubits n. For the case of the two-dimensional toric code [60], the radius satisfies $\ell = \Theta(\sqrt{n})$, so the effective rate is suppressed in number of qubits if the recovery rate scaling satisfies $\kappa = \omega(\sqrt{n})$.

The result we presented above can be improved for certain families of codes and recovery maps defined on n qubits. In this case, we can introduce an integer function $h = h(n)$ to be *the tolerable error weight* if the fraction of non-faithful trajectories of length $|\boldsymbol{\mu}| \leq h$ is at most $2^{-\Omega(d)}$, where d is the code distance[3]. For all codes, error weights below error radius ℓ are tolerable by definition. For a code family with a code capacity threshold $0 < f_c < 1$ [19], the maximum tolerable error weight is given by $h = \lfloor f_c n \rfloor$, typically greater than error radius ($h \geq \ell$). This allows us to improve the upper bound in Eq. (20) by replacing ℓ with h, where h stands for any tolerable error weight, and taking into account the exponentially small contribution in d coming from uncorrectable trajectories,

$$s(t) = \sum_{k=0}^{h} R(k, N\Delta t) - 2^{-\Omega(d)}. \tag{24}$$

This improvement grants us a stronger estimate for the logical error in the form

$$\Delta_{\mathrm{eff}} = \frac{\kappa}{\left(1 + \frac{\kappa}{N\Delta} \right)^{h+1}} + 2^{-\Omega(d)}. \tag{25}$$

---

[2]Here and below we use the family of "big-O" Bachmann-Landau notations: $o(f(x))$ (dominated by $f(x)$), $O(f(x))$ (bounded from above by $f(x)$), $\Theta(f(x))$ (bounded from below and above by $f(x)$), $\Omega(f(x))$ (bounded from below by $f(x)$), and $\omega(f(x))$ (dominates $f(x)$). More about definitions can be found in Ref. [59].

[3]For a more technical definition of the threshold and the tolerable error weight, we refer the reader to Appendix D.

In a similar fashion to the analysis in Eq. (23), if a code family has a tolerable weight $h > \ell$, we can use Eq. (25) to derive the bound

$$\Delta_{\text{eff}} = \kappa \exp\left(-\Theta(\kappa h/n\Delta)\right) + 2^{-\Omega(d)}, \qquad \kappa = o(n). \tag{26}$$

For example, the toric code has a threshold error weight $h = \Theta(n)$, which leads us to the error rate $\Delta_{\text{eff}} \propto \exp(-\Theta(\kappa/\Delta))$. Thus, a constant κ yields a constant memory time, while $\kappa \propto \log(n)$ yields a polynomial memory time.

These results are non-perturbative in Δ, as perturbation theory would predict that the logical error rate scales as order $O(\Delta^w)$ for some $w \geq 1$. We demonstrate this difference between our treatment and perturbation theory using the example of the toric code in Section 5.

Our bounds on autonomous error correction may seem surprising when compared to the standard scheme based on intermittent rounds of error-correcting recoveries. In the standard scheme, it is sufficient to maintain a constant ratio between the single-qubit error rate Δ and a fixed inverse time T^{-1} between recoveries in order to achieve an exponential lifetime. Indeed, if $nT\Delta < h$, the probability of accumulating more than h errors becomes exponentially small in n. The main difference between the two cases, stemming from our interpretation of autonomous recovery as a stochastic process, is that the time T between two consecutive recoveries is *not* fixed for the autonomous case and is instead determined by the Poisson distribution. Due to this fact, even for large κ, the probability that $n\Delta T > h$ is constant as a function of system size, although it is exponentially small in κ/Δ. Therefore, increasing the system size alone does not increase the lifetime of the logical qubit.

3.2   All-time bound

In the previous section, we derived an asymptotic estimate for $p(t)$ valid for $\kappa t \gg 1$. In this section, we present a rigorous upper bound on $p(t)$ and hence, by Lemma 1, on the logical error probability. This bound is valid for all times t and is summarized by the following Theorem.

Theorem 2. *Consider a family of n-qubit error-correcting codes for increasing n. Each code has a codespace C with code distance $d = d(n)$, a Poissonian noise model $\{E_\mu\}$, a recovery map $\mathcal{R}$ and a tolerable error weight $h = h(n)$. Then there exists a small parameter $\xi = 2^{-\Omega(d)}$ such that the logical error probability for the global decoder in Eq. (18), for any $t \geq 0$, satisfies*

$$\epsilon(t) \leq 1 - \exp\left(-(1-\xi)N\Delta\left(\frac{N\Delta}{\kappa + N\Delta}\right)^h t - \xi(\kappa + N\Delta)t\right). \tag{27}$$

We define the tolerable error weight precisely and provide a proof of the theorem in Appendix D. Similar to the asymptotic estimate in Section 3.1, the proof utilizes the Poissonian picture.[4] It uses the fact that the dynamics of the system is an ensemble average over trajectories where the single-shot recovery and the errors happen stochastically. Along a given

---

[4]It is worth noting that this bound holds for a more generic class of errors: instead of requiring $E_\mu^\dagger E_\mu = 1$ for all μ, the jump operators only have to satisfy $\sum_\mu E_\mu^\dagger E_\mu = N$. This class of errors also has the same convenient properties as the Poissonian model (16). Thus, the bound also applies in situations involving non-unitary errors such as those described by Pauli ladder operators $\sigma^\pm = (X \pm iY)/2$, provided $\sum_\mu E_\mu^\dagger E_\mu = N$.
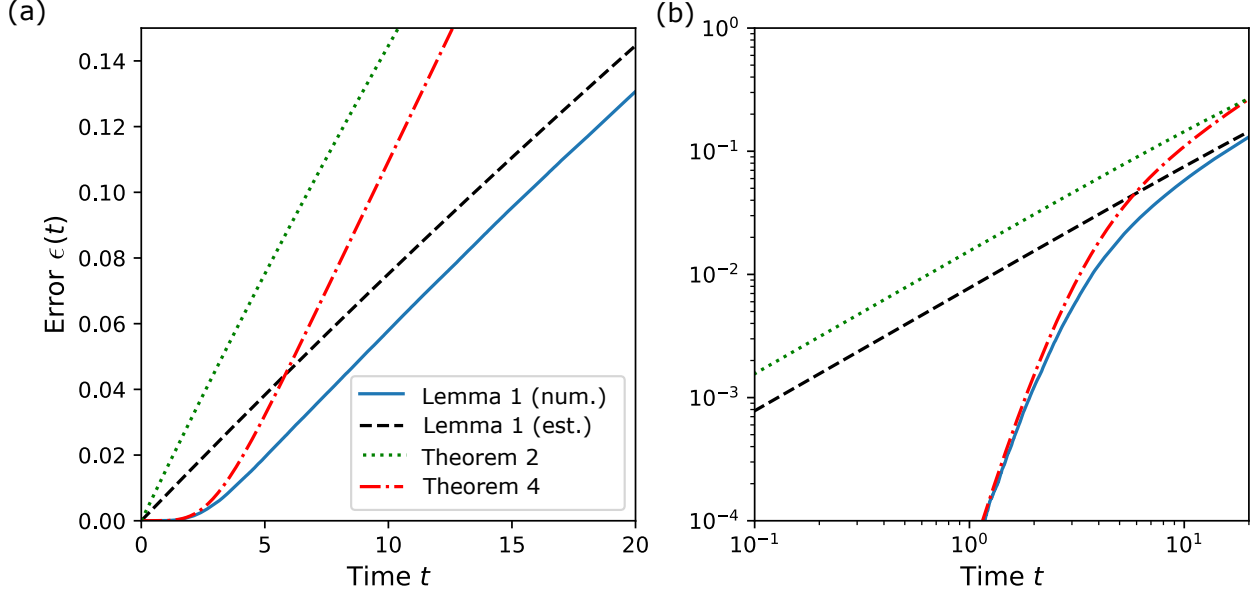
Figure 3: **Comparing the bounds for a Poisson error model**. The bounds on the logical error $\epsilon(t)$ as a function of time for a code with radius $\ell = 6$ and a recovery-to-noise ratio $\kappa = N\Delta = 1$. The plots compare numerically evaluated value of $p(t)$ in Eq. (18) (solid blue line) with its analytical asymptotic estimate in Eq. (21) (dashed black line), as well as the all-time bound in Eq. (27) (dotted green line) and the bound in Eq. (31) (dash-dotted red line). Panel (a) shows the linear scale, while panel (b) shows the logarithmic scale.

trajectory, the occurrence of a recovery event resets the system back to the codespace. If no more than h errors take place between any such consecutive resets, the recovery is almost guaranteed to send the system back to the correct codeword (up to a small failure rate ξ). We can therefore obtain an upper bound for the logical error probability by lower bounding the probability of trajectories consisting of only such faithful resets.

Consider an ideal recovery map that corrects only errors within the error radius, i.e. a tolerable error weight $h = \ell$ and $\xi = 0$. It therefore follows that

$$\epsilon(t) \leq 1 - \exp\left(-\frac{N\Delta t}{(1 + \kappa/N\Delta)^\ell}\right). \tag{28}$$

Comparing this rigorous all-time bound to the asymptotic estimate in Eq. (22), the all-time bound exceeds the estimate by a factor of $1 + N\Delta/\kappa$. This upper bound is also shown in Fig. 3.

Let us consider a particular class of Pauli-type noise models, where the Hermitian elementary error operators in Eq. (2) satisfy $E_\mu^2 = I$ and $E_\mu E_{\mu'} = \pm E_{\mu'} E_\mu$ for all μ, μ'. For example, we can consider a noise model where, at each qubit, the error is described by the same single Pauli jump operator, i.e. for a site i the error operator is $E_i = c_x X_i + c_y Y_i + c_z Z_i$ where $c_x, c_y, c_z \in \mathbf{R}$ and $c_x^2 + c_y^2 + c_z^2 = 1$. Another Pauli-type model is depolarizing noise, where the errors at each site i are described by three Pauli jump operators, $E_{3i+1} = X_i$, $E_{3i+2} = Y_i$, and $E_{3i+3} = Z_i$, where $i = 0, \ldots, n - 1$. The total number of error channels is given by $N = n$

13

and $N = 3n$ in the first and the second examples, respectively. Because error operators mutually commute or anticommute and their square is identity, two identical errors in the sequence cancel the effect of each other leading to a slightly better logical error scaling.

Theorem 3. *Under the conditions of Theorem 2 and for Pauli-type noise model, the logical error in Eq. (18) satisfies*

$$\epsilon(t) \leq 1 - \exp\left(-(1-\xi)N\Delta s_1 t - \xi(\kappa + N\Delta)t\right), \tag{29}$$

where s_1 is the solution to the recurrence relation

$$s_v = \frac{v}{N}p_1 s_{v-1} + \left(1 - \frac{v}{N}\right)p_1 s_{v+1}, \ \ s_0 = 0, \ \ s_{h+1} = 1, \tag{30}$$

with $p_1 = N\Delta/(\kappa + N\Delta)$.

The proof is similar to that of Theorem 2 and is given in Appendix E, where we also give a precise definition for the tolerable error weight h for the Pauli-type noise. The recurrence relation corresponds to a classical random walk, where a left or right move corresponds to an application of an error operator that increases or reduces the weight of the resulting total error[5].

We analyze the recurrence relation in Eq. (30) numerically. In particular, we compute s_1 for different κ and Δ, also varying N up to 10^7 (see Appendix E for the numerical results). We have the following empirical observations:

1. For $0 < h/N < 1/2$, we find that $\log s_1 \propto -\frac{\kappa}{\Delta}$ for $N \gg 1$.

2. For $h/N = 1/2$, we find that $\log s_1 \sim -\frac{\kappa}{4\Delta} \log N$ for $N \gg 1$.

For generic codes satisfying $h/N < 1/2$, the Pauli-noise bound in Theorem 3 yields an error rate lower than that of the general-noise bound in Theorem 2. In the special case when $h/N = 1/2$, Theorem 3 predicts a memory lifetime that increases as $N^{\kappa/4\Delta-1}$ when $\kappa > 4\Delta$. This case applies, for example, to the classical repetition code subject to the single-qubit bit-flip noise or the surface code subject to only qubit-erasure noise [61] or only Pauli-Y noise [62]. While the bound in Theorem 1 fails to capture it, Theorem 2 predicts an unbounded lifetime as $N \to \infty$ when $\kappa > 4\Delta$.

3.3 Logical error bound that is tight for early times

Applying the bound we found in Eq. (27) for early times indicates that $\epsilon(t) = O(t)$. However, numerical simulations shown in Fig. 5 suggest that linear scaling is only relevant at late times. Below, we establish a complementary bound $\epsilon(t) = O(t^{\ell+1})$ that confirms the slower-than-linear growth at early times. This bound also applies to the trace distance $\delta(t)$.

---

[5]Here, we count the error weight after cancelling all the repeating errors in a jump trajectory described by a string of elementary errors (Eq. (3)).

Theorem 4. *For Poissonian models in Eq. (16), the logical error rate is bounded as*

$$\epsilon(t), \delta(t) \leq \frac{1}{(1 + \kappa/N\Delta)^{\ell+1}} F_\ell\Big((\kappa + N\Delta)t\Big), \tag{31}$$

where $F(x)$ is defined in Theorem 1.

The proof of this result can be found in Appendix F. It follows the same steps as the proof of Theorem 1, with a slightly different resummation procedure made possible by the Poissonian error assumption. Since $\|\mathcal{L}_E\| \leq N$ for $\mathcal{L}_E$ that consists of N independent processes with unitary jumps, this yields a bound that improves on Theorem 1 by a factor at most $(1 + N\Delta/\kappa)^{\ell+1}$ for the case of a Poissonian error model.

The result from Theorem 4 provides an accurate scaling for the logical error at early times, while also capturing the error rate at later times. In the limit $x \to 0$, we observe the scaling $F_\ell(x) \propto x^{\ell+1}$. On the other hand, when $x \gg 1$, this function behaves as $F_\ell(x) \propto x$. This means that the error rate at early times grows as $\epsilon(t) \propto (tN\Delta)^{\ell+1}$ and saturates to a linear rate. In the late-time regime, the logical error satisfies

$$\epsilon(t) \leq \left(\frac{N\Delta}{\kappa + N\Delta}\right)^{\ell+1} (\kappa + N\Delta)t = \frac{N\Delta t}{(1 + \kappa/N\Delta)^\ell}. \tag{32}$$

Thus, this bound is consistent with the Taylor expansion of the bound in Eq. (28) if the logical error rate is small. It is also illustrated in Fig. 3 along with the bounds we derived previously.

4 Lower bound: qubit stabilizer codes

The above upper bounds on the logical error rate scale no faster than $N \exp(-c\kappa/\Delta)$ in the recovery rate κ, saturating at $\exp(-c'\kappa/\Delta)$ when $\kappa t \gg 1$ (for some positive constants c, c'). This leaves the possibility that, for some times, global decoders may be able to suppress errors more efficiently. However, using the example of qubit stabilizer codes [2, 63] subject to single-qubit Pauli errors, we show below that this is generally not the case. We derive a *lower bound* on the error rate that decreases exponentially with the recovery-to-noise ratio κ/Δ, and is independent of the number of qubits n. In other words, it is impossible to reduce the logical error rate to zero in the $n \to \infty$ limit while maintaining a constant recovery rate.

Our lower bound applies to single-qubit Pauli noise and logical-qubit stabilizer codes with the following two additional natural features:

1. There exists a timescale after which the logical information gets corrupted with nonzero probability. In other words, in the absence of recovery, the noise generates a nonzero probability of a logical flip,

$$\alpha(\tau) := \text{Tr}\Big(|1\rangle\langle 1|\mathcal{R}e^{\mathcal{L}_{\kappa=0}\tau}|0\rangle\langle 0|\Big) > 0 , \tag{33}$$

for times $\tau > \tau_c \propto 1/\Delta$, where $\mathcal{L}_{\kappa=0}$ is the generator of noisy evolution without any recovery ($\kappa = 0$) and $|w\rangle$ are the logical states. The threshold time τ_c is size-independent
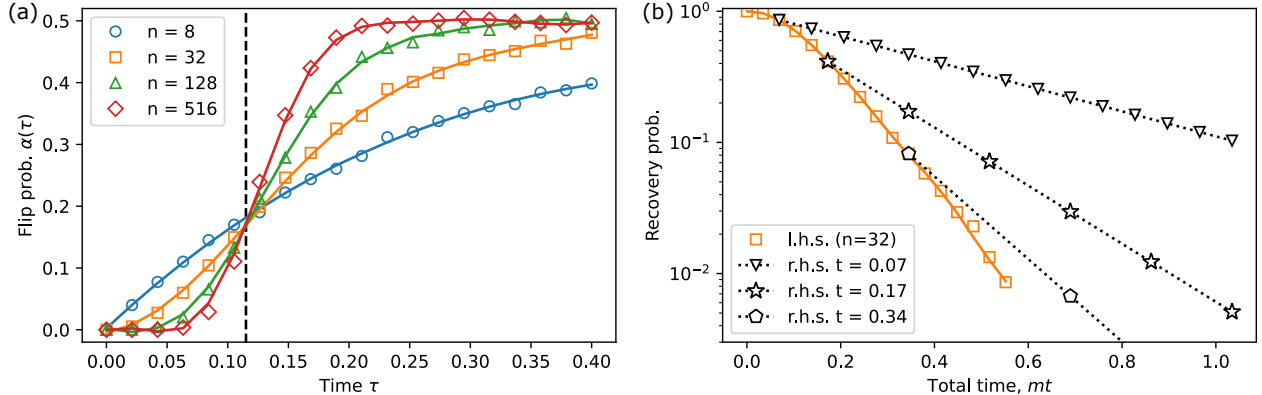
Figure 4: **Logical error after recovery for 2D toric code.** Here, we put $\Delta = 1$ and consider only bit-flip errors $E_\mu \equiv X_\mu$, where μ enumerates the physical qubits. We utilize the recovery map $\mathcal{R}$, based on the minimum-weight-matching algorithm (see Section 5 for details). (a) The flip probability $\alpha(\tau)$ in Eq. (33) in the absence of recovery ($\kappa = 0$) for a different number of spins on a square lattice. Dots represent numerical data for the $L \times L$ lattice (the total number of qubits $n = 2L^2$ given in the legend), lines are smooth interpolations. For times larger than $\tau_c \approx 0.115$, marked by a dashed line, the logical flip probability is always nonzero, approaching the value of 0.5 for large codes. (b) Comparison of the recovery probabilities for $n = 32$ qubits in two cases: (i) a single recovery at the end, as given by the left-hand side of Eq. (34) (orange dots), and (ii) repeated recoveries, as given by the right-hand side, for different times t (dotted curves) and different numbers of recoveries m (white triangles, stars, and pentagons). For all parameters, repeated recoveries in case (ii) perform better than applying the final recovery only in case (i).

and sets the timescale after which the logical information is no longer perfectly recoverable. For generic Pauli noise, the function $\alpha(\tau)$ also depends on system size and is assumed to satisfy $\lim_{n \to \infty} \alpha(\tau) = 1/2$ for $\tau > \tau_c$. This ensures that the noise model is sufficiently powerful. In Fig. 4(a), we illustrate this property by plotting $\alpha(\tau)$ for different system sizes of the 2D toric code (see Section 5 for a definition). In this plot, one can clearly observe the threshold time τ_c after which the logical state appears highly mixed after the recovery map for any size of the code.

2. Interleaving the noise with more recovery operations is more effective. More technically, the probabilities of recovery satisfy

$$\mathrm{Tr}\left[|0\rangle\langle 0|\mathcal{R}e^{\mathcal{L}mt}|0\rangle\langle 0|\right] \leq \mathrm{Tr}\left[|0\rangle\langle 0|\left(\mathcal{R}e^{\mathcal{L}t}\right)^m|0\rangle\langle 0|\right] \qquad (34)$$

for any time $t \geq 0$ and integer $m \geq 0$. We illustrate this property in Fig. 4(b) for the 2D toric code. Specifically, we plot both the right-hand side and the left-hand side of this inequality for different times t and integers m. Notably, this inequality holds even at times $t > \tau_c$, when the average probability of errors for each physical qubit exceeds the code threshold. While we do not generally expect good performance from the decoder in this case, the toric code demonstrates some improvement even above the threshold.

16

Given these assumptions, we can show the existence of the minimal logical error rate. To do so, let us first consider the logical bit-flip probability in the presence of the recovery process. Let $F^{(0)}$ be the subset of trajectories without any recovery events (i.e., the $\kappa = 0$ case only), a subset of all possible trajectories F. From the Poissonian picture in Eq. (16), we derive that

$$
\begin{aligned}
\mathrm{Tr}\left[|1\rangle\langle 1|\mathcal{R}e^{\mathcal{L}\tau}|0\rangle\langle 0|\right] &= \mathrm{Tr}\left[|1\rangle\langle 1|\mathcal{R}\left(\sum_{\boldsymbol{\mu}\in F} p(\boldsymbol{\mu},\tau)\mathcal{E}_{\boldsymbol{\mu}}\right)|0\rangle\langle 0|\right] \\
&\geq \mathrm{Tr}\left[|1\rangle\langle 1|\mathcal{R}\left(\sum_{\boldsymbol{\mu}\in F^{(0)}} p(\boldsymbol{\mu},\tau)\mathcal{E}_{\boldsymbol{\mu}}\right)|0\rangle\langle 0|\right] \\
&= \mathrm{Tr}\left[|1\rangle\langle 1|\mathcal{R}\left(\sum_{\boldsymbol{\mu}\in F^{(0)}} p(\boldsymbol{\mu},\tau)\right)\left(\sum_{\boldsymbol{\mu}\in F^{(0)}} \frac{p(\boldsymbol{\mu},\tau)}{\sum_{\boldsymbol{\mu}'\in F^{(0)}} p(\boldsymbol{\mu}',\tau)}\mathcal{E}_{\boldsymbol{\mu}}\right)|0\rangle\langle 0|\right] \\
&= e^{-\kappa\tau}\mathrm{Tr}\left[|1\rangle\langle 1|\mathcal{R}e^{\mathcal{L}_{\kappa=0}\tau}|0\rangle\langle 0|\right] \geq \alpha(\tau)e^{-\kappa\tau},
\end{aligned}
\tag{35}
$$

indicating a non-vanishing error probability in the thermodynamic limit. Here, we used the normalization

$$
\sum_{\boldsymbol{\mu}\in F^{(0)}} p(\boldsymbol{\mu},\tau) = \sum_{k=0}^{\infty}\left(\frac{N\Delta}{\kappa+N\Delta}\right)^k \frac{[\tau(\kappa+N\Delta)]^k}{k!}e^{-\tau(\kappa+N\Delta)} = e^{-\kappa\tau}.
\tag{36}
$$

Using Eq. (34), we then lower bound the logical error measure by considering the dynamics interleaved with the recovery map at every time interval of length τ.

Let the parity superoperators be $\mathcal{X}(\rho) = \bar{X}\rho\bar{X}$ and $\mathcal{Z}(\rho) = \bar{Z}\rho\bar{Z}$, where $\bar{X}$ and $\bar{Z}$ are the logical operators. For stabilizer codes, these operators are Pauli strings that commute with the stabilizers. Also, the recovery $\mathcal{R}$ can be written in terms of projectors onto Pauli stabilizer configurations followed by Pauli strings that fix the stabilizer configuration (see Section 5 for an explicit expression). These superoperators satisfy $[\mathcal{R},\mathcal{X}] = [\mathcal{R},\mathcal{Z}] = 0$. Similarly, for Pauli errors $\mathcal{E}_{\mu>0}$, we have

$$
\mathcal{X}\mathcal{E}_{\mu}(\rho) = \mathcal{X}(E_{\mu}\rho E_{\mu}) = E_{\mu}\mathcal{X}(\rho)E_{\mu} = \mathcal{E}_{\mu}\mathcal{X}(\rho) ,
\tag{37}
$$

and similarly for $\mathcal{X} \to \mathcal{Z}$. As a result, the parity operators are conserved during the dynamics, i.e. $[\mathcal{X},e^{\mathcal{L}t}] = [\mathcal{Z},e^{\mathcal{L}t}] = 0$.

To analyze the logical error rate of our system, we limit our attention to the initial state $|0\rangle\langle 0|$. This state is an eigenvector of the parity operator $\mathcal{Z}$ with eigenvalue $+1$. Its eigenvalue is a good quantum number with respect to the noise, meaning that no off-diagonal matrix elements (such as $|0\rangle\langle 1|$) will be created during the evolution. Combining this with Eq. (35) for sufficiently large n, we have

$$
\mathcal{R}e^{\mathcal{L}\tau}|0\rangle\langle 0| = p_0|0\rangle\langle 0| + p_1|1\rangle\langle 1|, \ \alpha(\tau)e^{-\kappa\tau} \leq p_1 \leq \frac{1}{2},
\tag{38}
$$

where $p_0 = 1 - p_1$. By applying $\mathcal{X}$ to both sides of Eq. (38), we learn that

$$
\mathcal{R}e^{\mathcal{L}\tau}|1\rangle\langle 1| = p_0|1\rangle\langle 1| + p_1|0\rangle\langle 0|.
\tag{39}
$$

17

Using simple linear algebra, we find:

$$\left(\mathcal{R}e^{\mathcal{L}\tau}\right)^m |0\rangle\langle 0| = \left(\frac{1}{2} + (1-2p_1)^m\right)|0\rangle\langle 0| + \left(\frac{1}{2} - (1-2p_1)^m\right)|1\rangle\langle 1|. \tag{40}$$

This yields

$$\mathrm{Tr}\left[|0\rangle\langle 0|\mathcal{R}\left(e^{\mathcal{L}\tau}\mathcal{R}\right)^m |0\rangle\langle 0|\right] \leq \frac{1}{2} + \frac{1}{2}(1-2\alpha(\tau)e^{-\kappa\tau})^m. \tag{41}$$

For a total time $t = m\tau$, we use Eq. (34) from Assumption 2 and arrive at the following bound,

$$\frac{1}{2} - \frac{1}{2}(1-2\alpha(\tau)e^{-\kappa\tau})^{t/\tau} \leq 1 - \mathrm{Tr}\left[|0\rangle\langle 0|\mathcal{R}e^{\mathcal{L}t}|0\rangle\langle 0|\right] \leq \epsilon(t). \tag{42}$$

To make this bound comparable to previous results, we rewrite this inequality as $\epsilon(t) \geq \frac{1}{2}(1 - \exp(-\Delta_{\mathrm{eff}}(t)t))$, where the effective logical error rate is

$$\Delta_{\mathrm{eff}}(t) := -\frac{1}{t}\log(1-2\epsilon(t)) \geq -\frac{1}{\tau}\log(1-2\alpha(\tau)e^{-\kappa\tau}) \approx \frac{2\alpha(\tau)}{\tau}e^{-\kappa\tau}, \tag{43}$$

The approximation in the last step is valid if $\alpha(\tau)e^{-\kappa\tau} \ll 1$. According to Assumption 1, the flip probability satisfies $\lim_{n\to\infty}\alpha(\tau) = 1/2$ for all $\tau > \tau_c = f'/\Delta$, where f' is a constant. Therefore, the effective error rate Δ_{eff} is $\Omega(\Delta e^{-f'\kappa/\Delta})$ as the thermodynamic limit is approached. This result shows that the lower bound on the logical error rate decreases exponentially as a function of the ratio between the recovery rate and the error rate. However, it also follows that, under the assumptions in Eqs. (33,34) (which we verified for the 2D toric code but expect to hold more generally), it is impossible to obtain a quantum memory with either an exponential or polynomial lifetime using only a constant recovery rate. Some careful readers may notice that Theorem 3 suggests that the repetition code subject to a single type of Pauli noise has a memory lifetime that grows polynomially with system size. This does not contradict the lower bound. One can verify numerically that Assumption 1 is violated by the repetition code, i.e., the timescale τ_c for logical information corruption under purely noisy dynamics grows with system size.

5   Examples of autonomous codes

Finally, we provide a few examples of autonomous codes generated from global decoders of existing quantum codes. We start with qubit stabilizer codes. Our *global* recoveries are different from local decoders [21,22,65,66] in that jump operators of the latter apply recovery steps only on geometrically restricted regions.

The codespace C of an $[[n,1,d]]$ stabilizer code is formed by the $+1$ eigenstates of $n-1$ mutually commuting Pauli operators S_α that satisfy $S_\alpha^2 = I$, $[S_\alpha, S_\beta] = 0$ for all α, β. The traditional recovery map includes two steps. In the first step, we measure all stabilizer generators S_α, projecting the state into a subspace of mutual eigenstates with corresponding eigenvalues $s_\alpha = \pm 1$. This procedure is equivalent to applying a projection operator

$$P(\mathbf{s}) = \prod_{\alpha=1}^{n-1} \frac{1}{2}\left(1 + s_\alpha S_\alpha\right). \tag{44}$$

18
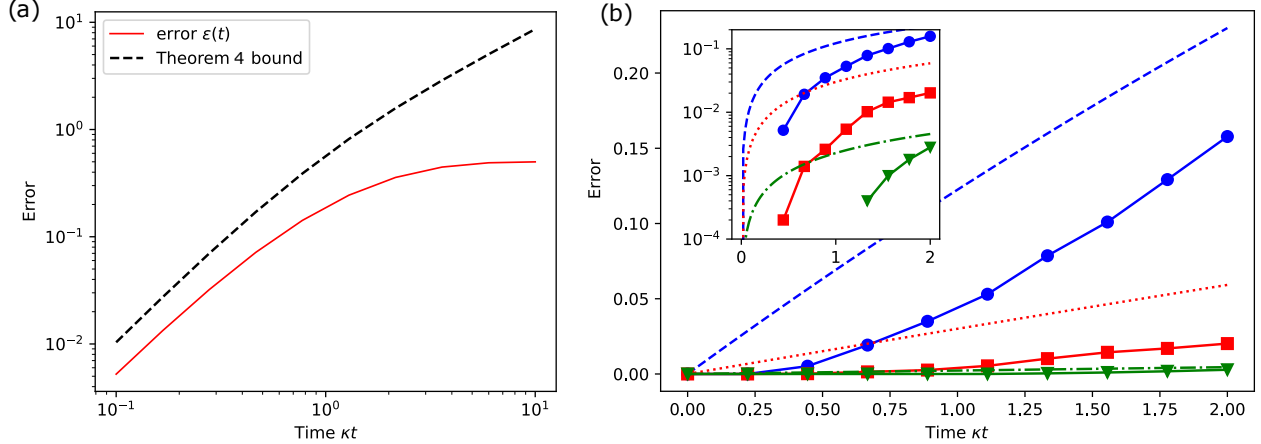
Figure 5: **Stabilizer codes.** (a) Logical error measure $\epsilon(t)$ for the five-qubit code and the corresponding upper bound in Eq. (31). (b) The same logical error measure for the two-dimensional toric code on a $L \times L$ lattice of linear sizes $L = 4$ (blue), 6 (red), and 8 (green), assuming the minimum-weight-matching algorithm has the threshold $h \approx 0.1031\, n$ [64]. The recovery rate grows linearly with the number of qubits, $\kappa = 0.1\, n$. The inset shows the same plot in logarithmic scale on the y-axis.

Next, we apply the corresponding recovery unitary $C(\boldsymbol{s})$, which is a product of individual Pauli operators, depending on the $(n-1)$-dimensional vector of outcomes $\boldsymbol{s} = \{s_\alpha\}$. We can make a decision on the recovery using an algorithm or simply a lookup table that pairs every stabilizer configuration with its corresponding recovery.

In the autonomous regime, we propose to implement these recoveries using the continuous process, which combines both procedures:

$$\mathcal{R}(\rho) = \sum_{\mathbf{s} \in \mathbb{Z}_2^{n-1}} A_{\mathbf{s}} \rho A_{\mathbf{s}}^\dagger, \tag{45}$$

where the jump operators are defined as

$$A_{\mathbf{s}} = C(\mathbf{s})P(\mathbf{s}) = PC(\mathbf{s}). \tag{46}$$

Here P is the projector onto the codespace, and the last equality follows from the fact that $C(\mathbf{s})$ commutes (anticommutes) with the stabilizer S_α if $s_\alpha = 1$ (-1):

$$C(\mathbf{s}) \prod_{\alpha=1}^{n-1} \frac{1}{2}\Big(1 + s_\alpha S_\alpha\Big) = \prod_{\alpha=1}^{n-1} \frac{1}{2}\Big(1 + S_\alpha\Big) C(\mathbf{s}) = PC(\mathbf{s}). \tag{47}$$

For these stabilizer recovery models, we use simplistic Pauli error operators $E_\mu \in \{X_i, Y_i, Z_i\}$ in Eq. (2), which act with the same rate Δ on each qubit i (i.e., we set all $\lambda_\mu = 1$).

In the simplest example, we consider an autonomous stabilizer decoder based on a five-qubit code. This distance $d = 3$ code protects one logical qubit using five physical qubits and is stabilized by four operators $S_\alpha \in \{XZZXI, IXZZX, XIXZZ, ZXIXZ\}$, where I, X, and Z are respectively the identity and the X- and Z-Pauli operators acting on the

19
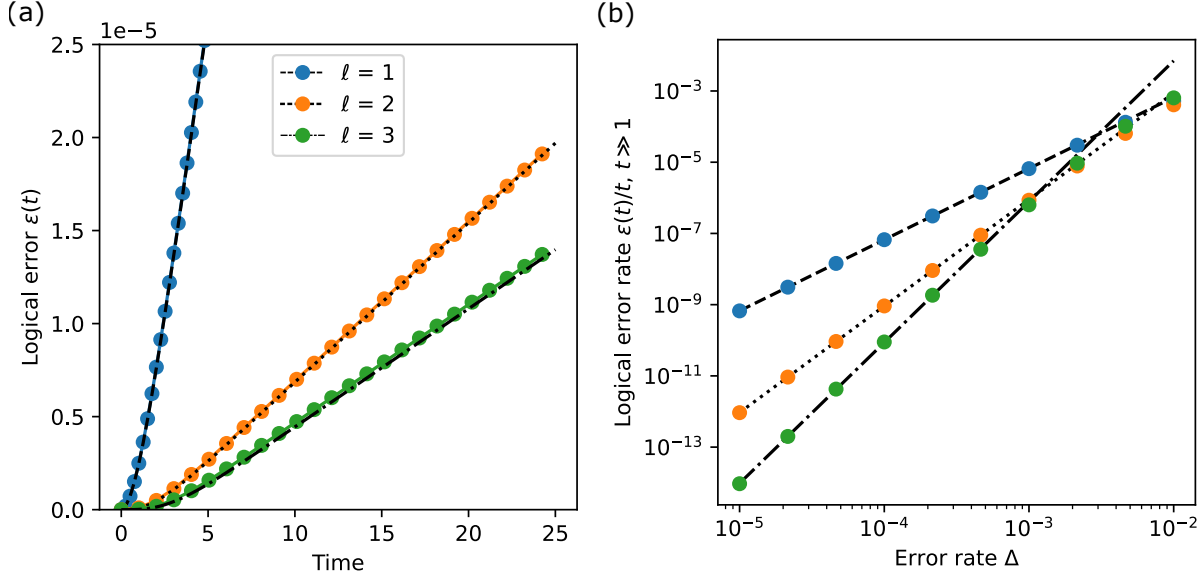
Figure 6: **Binomial code.** (a) The error probability $\epsilon(t)$ in Eq. (11) for the binomial code in Eq. (51) with different values of $\ell = 1, 2, 3$ using the parameters $\kappa = 1$, $\Delta = 10^{-3}$. The dots show numerical results (obtained for finite-size Hilbert space approximation), the curves show the fit of the form $\epsilon(t) = (c_\ell \Delta)^{\ell+1} F(\kappa t)$ (compare to the result in Theorem 1), where $c_1 = 2.57$, $c_2 = 9.50$, and $c_3 = 28.2$. (b) The dots show the saturated error rate for different values of ℓ as a function of Δ. The curves show the asymptotics of the form $\epsilon(t) = (c'_\ell \Delta)^{\ell+1} t$, where $c'_1 = 2.57$, $c'_2 = 9.51$, and $c'_3 = 28.54$. This agrees with the theoretical bound in Eq. (13) when taking into account that $\|\mathcal{L}_E\|_\mathsf{K} \geq C_\ell > c_\ell, c'_\ell$, where $C_\ell := \sqrt{\mathrm{Tr}\left(|0\rangle\langle 0|\mathcal{L}_E^\dagger \mathcal{L}_E |0\rangle\langle 0|\right)}$, $|0\rangle$ is ℓ-dependent codeword in Eq. (51), and $C_1 \approx 6.50$, $C_2 \approx 24.5$, and $C_3 \approx 61.0$.

corresponding qubit of the system. We illustrate the performance of this code in Fig. 5(a). As can be seen from the figure, the upper bound in Eq. (31) accurately describes the error rate in such a model.

Another relevant example is the two-dimensional toric code. This code is defined on a two-dimensional square lattice with $L \times L$ plaquettes and periodic boundary conditions, where physical qubits are situated on the edges. The stabilizers are divided into two groups. One group includes all products of four Z operators acting on edges s adjacent to a vertex ("stars"), which we denote as $A_s = \prod_{i \in s} Z_i$. The other group consists of all products of X operators acting around a square p ("plaquettes"), which we denote as B_p. The codespace consists of the ground states of the operator

$$H = -\sum_s A_s - \sum_p B_p. \tag{48}$$

Using measurements of each group of stabilizers separately, it is possible to independently correct errors in the X and Z bases even if both of them are present in the system. To construct the recovery operator $\mathcal{R}$, we use the minimum-weight-matching algorithm [64], which suggests the recovery unitary $C(\mathbf{s})$ for each vector of measurement outcomes $\mathbf{s}$. We compare the rate of logical error with the prediction given by the upper bound from Theorem 2. In

particular, Fig. 5(b) shows how the logical error depends on the linear size L of the lattice. It can be seen that the upper bound correctly predicts the performance of the code.

Additionally, we compare our results with the predictions of perturbation theory for the autonomous toric code model. First, we find the solution of the spectral problem exactly for a Lindbladian with no noise ($\Delta = 0$). This solution has a 4^2-dimensional steady-state manifold that is separated by a dissipative gap κ from the rest of the eigenstates. The steady states are superpositions of four toric-code ground states. The rest of the eigenstates have the same eigenvalue κ. Using this exact solution, we use perturbation theory to determine how the eigenvalues of steady states are perturbed by noise. The real part of the lowest-order perturbation can be used as an estimate of the logical error rate.

Notably, as we show in Appendix H, when κ is a system-size independent constant, the leading-order contribution from perturbation theory diverges as L approaches infinity. If the recovery rate scales with L as $\kappa = \kappa_0 L$ for some constant $\kappa_0 > 0$, the leading-order contribution from perturbation theory scales as

$$\epsilon(t) = O\left(\kappa_0 t L^2 \left(\frac{2\Delta}{e\kappa_0}\right)^{L/2}\right) \tag{49}$$

in the limit $L \to \infty$. This still provides a better estimate than that for the general recovery process in Theorem 1, which requires $\kappa \sim L^2$ to ensure exponential suppression of the logical error rate. As a comparison, we can apply the asymptotic result obtained in Section 3.1 to the autonomous toric code by setting $N = n = 2L^2$ and $h = 2fL^2$ for some constant $f > 0$ that indicates the finite threshold of the toric code. The error rate given by Eq. (25) is

$$\epsilon(t) = O\left(\kappa_0 t L e^{-f\kappa_0 L/\Delta}\right), \tag{50}$$

which suggests a non-perturbative contribution at $\Delta = 0$. Indeed, we see that, although the perturbation result does capture the exponential suppression of the error rate as L approaches infinity, for small Δ it overestimates the error rate compared to the asymptotic behaviour. This example highlights the importance of non-perturbative approaches in estimating the memory lifetime for an autonomous error-correcting code.

Finally, we consider an example of a code that cannot be understood in terms of Pauli errors. An example of such a code is the binomial code [67] defined for the space of a quantum harmonic oscillator, $\mathsf{H} = \{|n\rangle_B, n \geq 0\}$. The transitions between quantized oscillator levels are induced by the creation operator $a^\dagger$ and the annihilation operator a such that $a^\dagger|n\rangle_B = \sqrt{n+1}|n+1\rangle_B$ and $a|n\rangle_B = \sqrt{n}|n-1\rangle_B$. The codewords of the binomial code of distance $d = 2\ell + 1$ are

$$|0\rangle, |1\rangle = \frac{1}{2^\ell} \sum_{s \in \text{even,odd}}^{[0,2\ell+1]} \sqrt{\binom{2\ell+1}{s}}|s(2\ell+1)\rangle_B. \tag{51}$$

The binomial code tolerates single-photon processes as well as dephasing, with elementary errors generated from the set $E_\mu \in \{a, a^\dagger, a^\dagger a\}$, where weights $\lambda_\mu = 1/3$ are the same for each channel type in Eq. (2). The recovery map $\mathcal{R}$ is defined using the procedure in Appendix A. Fig. 6 shows that the logical error rate of the code decreases exponentially with the code radius, for different values of ℓ.

6 Summary and outlook

We derived the universal dependence of the logical error of a global quantum decoder on error model parameters. Under general assumptions, we found that global decoders provide viable error suppression. We also developed criteria under which the lifetime of the memory can be extended indefinitely by increasing the system size. To achieve this, decoders must operate at a rate that grows with system size. While this growth can be mild—polynomial suppression can be achieved with logarithmic rates—it shows that a constant dissipative gap of the recovery procedure is not sufficient to ensure a quantum memory whose lifetime grows indefinitely with system size. It also means, contrary to what one might naively imagine, that autonomous decoders cannot be perceived or constructed as stochastic versions of traditional error correction protocols. In fact, the structure of the correction map (e.g., represented by $\mathcal{K}_t$ in Eq. (6)) plays an important role in existing autonomous decoders [21].

Another motivation for studying non-local dissipative processes is to see if they exhibit threshold-like behavior. While we do not generally observe sharp features like this in our analytical analysis of Poissonian models, it is possible that a transition could occur for a more general type of noise model that becomes weaker as system size increases.

In the future, we could use similar techniques to study local decoders. For example, we could try to prove analytically that there is a threshold for autonomous models based on existing cellular-automata decoders such as sweep-rule decoders [68] or local decoders motivated by the thermalization of physical Hamiltonians [22].

Acknowledgments

Appendices

Appendix A: Recovery map and error measures

In this appendix, we show how the map $\mathcal{R}$ in Eq. (6) can be constructed explicitly for a given quantum code. We also show the connections between two error measures introduced in Eqs. (10) and (11).

We start by explicitly constructing the recovery map and proving some of its properties. To do so, we first consider the error operators $F_\alpha = \sum_\nu u^*_{\alpha\nu} K_\nu$, where $u_{\alpha\nu}$ are matrix elements of the unitary u that diagonalizes the matrix C in Eq. (4), i.e. $C = u^\dagger \hat{C} u$, where $\hat{C} = \mathrm{diag}\{d_\alpha\}$. The action of these operators is orthogonal in the codespace, i.e.

$$PF_\alpha^\dagger F_\beta P = d_\alpha \delta_{\alpha\beta} P, \tag{52}$$

where P is the projector to the codespace C and d_α are eigenvalues of C. We will only consider independent operators with $d_\alpha > 0$. Next, we can use the polar decomposition

$$F_\alpha P = U_\alpha \sqrt{PF_\alpha^\dagger F_\alpha P} = \sqrt{d_\alpha} U_\alpha P, \tag{53}$$

where U_α are unitary operators. Then, we can construct the recovery map as

$$\mathcal{R}(\rho) = \sum_{\alpha=1}^{D_0} R_\alpha \rho R_\alpha^\dagger + \frac{1}{2}\mathrm{Tr}\,(\rho P_\perp) P \qquad R_\alpha = P U_\alpha^\dagger, \tag{54}$$

where $P_\perp = I - \sum_\alpha R_\alpha^\dagger R_\alpha$ is the projector on the sector of "undecidable" error states created by acting on the codespace by errors that violate Knill-Laflamme condition. Here, R_α are Kraus operators that satisfy the property

$$R_\alpha R_\beta = P U_\alpha^\dagger P U_\beta^\dagger = \frac{1}{\sqrt{d_\alpha}} P F_\alpha^\dagger P U_\beta^\dagger = \delta_{\alpha 0} R_\beta, \tag{55}$$

where $F_0 = I$ and $d_0 = 1$. This form of recovery map is not the most general one, as one could advise a better code-specific map that addresses undecidable states. For the sake of simplicity, however, we limit ourselves to the simple map presented above.

Using the relation in Eq. (55), we can show that the recovery map is an idempotent operation, i.e.

$$\forall \rho: \quad \mathcal{R}^2(\rho) = \sum_{\alpha\beta=1}^{D_0} R_\alpha R_\beta \rho R_\beta^\dagger R_\alpha^\dagger + \frac{1}{2}\mathrm{Tr}\,(\rho P_\perp) P = \mathcal{R}(\rho). \tag{56}$$

Finally, using the structure of the Kraus operators in Eq. (54), we can derive its action on error states as

$$\forall \rho \in \mathsf{L}(\mathsf{C}): \quad \mathcal{R}(F_\alpha \rho F_\beta^\dagger) = \sum_\gamma P U_\gamma^\dagger F_\alpha \rho F_\beta^\dagger U_\gamma P = \sum_\gamma \frac{1}{d_\gamma} P F_\gamma^\dagger F_\alpha P \rho P F_\beta^\dagger F_\gamma P, \tag{57}$$

where $\mathsf{L}(\mathsf{C})$ is the space of linear operators on the codespace C. Using the Knill-Laflamme condition, we get the expression

$$\forall \rho \in \mathsf{L}(\mathsf{C}): \quad \mathcal{R}(F_\alpha \rho F_\beta^\dagger) = \sum_\gamma d_\gamma \delta_{\alpha\gamma} \delta_{\beta\gamma} \rho = d_\alpha \delta_{\alpha\beta} \rho. \tag{58}$$

Transforming back to the error basis consisting of individual errors, we get

$$\forall \rho \in \mathsf{L}(\mathsf{C}): \quad \mathcal{R}(K_{\boldsymbol{\mu}} \rho K_{\boldsymbol{\nu}}^\dagger) = C_{\boldsymbol{\nu}\boldsymbol{\mu}} \rho. \tag{59}$$

This relation is important: we will use it for proving the properties of the recovery map in Appendix B.

Next, we present a proof of the relationship between the trace distance and the fidelity measures of logical error, defined in Eqs. (10) and (11). In particular, we show that

$$\delta(t) \le 2\epsilon(t). \tag{60}$$

The first step is to utilize Holder's inequality, namely

$$T(\exp(\mathcal{L}t)\rho_0, \exp(\mathcal{L}t)\rho_0^\perp) \ge \frac{1}{2} \text{Tr}\left(Q \exp(\mathcal{L}t)\delta\rho_0\right), \tag{61}$$

where $\delta\rho_0 = \rho_0 - \rho_0^\perp$, and Q is any Hermitian operator of unit spectral norm. It is convenient to choose $Q = \mathcal{R}^\dagger \delta\rho_0$, where $\mathcal{R}^\dagger$ is the adjoint to the recovery operator $\mathcal{R}$. Then

$$\begin{aligned}
T(\exp(\mathcal{L}t)\rho_0, \exp(\mathcal{L}t)\rho_0^\perp) &\ge \frac{1}{2} \text{Tr}\left(\delta\rho_0 \mathcal{R} \exp(\mathcal{L}t)\delta\rho_0\right) \\
&= \text{Tr}\left(\rho_0 \mathcal{R} \exp(\mathcal{L}t)\rho_0\right) + \text{Tr}\left(\rho_0^\perp \mathcal{R} \exp(\mathcal{L}t)\rho_0^\perp\right) - 1,
\end{aligned} \tag{62}$$

where we use that $\rho_0 + \rho_0^\perp = I_C$, I_C acts as identity within the codespace and zero outside of it. Incorporating this inequality into the definition of $\delta(t)$, we get

$$\begin{aligned}
\delta(t) &\le 2 - \min_{\rho_0}\left(\text{Tr}\left(\rho_0 \mathcal{R} \exp(\mathcal{L}t)\rho_0\right) + \text{Tr}\left(\rho_0^\perp \mathcal{R} \exp(\mathcal{L}t)\rho_0^\perp\right)\right) \\
&\le 2\left(1 - \min_{\rho_0} \text{Tr}\left(\rho_0 \mathcal{R} \exp(\mathcal{L}t)\rho_0\right)\right) = 2\epsilon(t).
\end{aligned} \tag{63}$$

This concludes our proof.

Appendix B: Proof of Theorem 1

This appendix contains the proof of Theorem 1. In the first step of the proof, we show that the error measures in Eqs. (11) satisfy

$$\epsilon(t), \delta(t) \le 1 - \frac{1}{2} \min_{\rho_0} \text{Tr}\left(Q \exp(\mathcal{L}t)\delta\rho_0\right), \tag{64}$$

where $\delta\rho_0 = \rho_0 - \rho_0^\perp$ and $Q = \mathcal{R}^\dagger \delta\rho_0$, similar to the notation we used in Appendix A. The inequality for $\delta(t)$ follows directly from its definition in Eq. (10) and the property in Eq. (61). To prove this inequality for $\epsilon(t)$, we notice that

$$\begin{aligned}
\frac{1}{2} \min_{\rho_0} \text{Tr}\left(Q \exp(\mathcal{L}t)\delta\rho_0\right) &= \min_{\rho_0}\left(\text{Tr}\left(\rho_0 \mathcal{R} \exp(\mathcal{L}t)\rho_0\right) + \text{Tr}\left(\rho_0^\perp \mathcal{R} \exp(\mathcal{L}t)\rho_0^\perp\right)\right) - 1 \\
&\le \min_{\rho_0} \text{Tr}\left(\rho_0 \mathcal{R} \exp(\mathcal{L}t)\rho_0\right) = 1 - \epsilon(t),
\end{aligned} \tag{65}$$

where we used the fact that $\mathrm{Tr}\,(\rho_0^\perp \mathcal{R}\exp(\mathcal{L}t)\rho_0^\perp) \leq 1$. This expression leads us to the inequality in Eq. (64) for $\epsilon(t)$.

Next, it is convenient to switch to the imaginary frequency space $t \to s$ and write this inequality using the inverse Laplace transform $\mathscr{L}^{-1}$ as

$$\epsilon(t), \delta(t) \leq 1 - \frac{1}{2}\min_{\rho_0} \mathscr{L}^{-1}\left[\mathrm{Tr}\left(Q\frac{1}{s-\mathcal{L}}\delta\rho_0\right)\right]. \tag{66}$$

To further analyze this expression, we use the decomposition $\mathcal{L} = \kappa\mathcal{L}_R + \Delta\mathcal{L}_E$, where $\mathcal{L}_E$ and $\mathcal{L}_R$ are defined in Eqs. (2) and (5), respectively. With error rate Δ as a small parameter, we are using Dyson's series

$$\frac{1}{s-\mathcal{L}} = \frac{1}{s-\kappa\mathcal{L}_R}\sum_{r=0}^{\infty}\left(\Delta\mathcal{L}_E\frac{1}{s-\kappa\mathcal{L}_R}\right)^r. \tag{67}$$

To simplify calculations, we can use diagrammatic notation to represent different superoperators. We introduce the following notation:

$$Q \otimes I \equiv \square, \qquad \frac{1}{s-\mathcal{L}} \equiv \text{\textit{eee}}, \qquad \frac{1}{s-\kappa\mathcal{L}_R} \equiv \text{==}, \qquad \Delta\mathcal{L}_E \equiv \otimes, \qquad \frac{1}{2}\mathrm{Tr}\,(\mathcal{O}\delta\rho_0) \equiv \langle\mathcal{O}\rangle. \tag{68}$$

Using this notation, the Dyson's series in Eq. (67) can be expressed as an infinite sum of diagrams,

$$\text{\textit{eee}} = \text{==} + \text{=⊗=} + \text{=⊗=⊗=} + \text{=⊗=⊗=⊗=} + \ldots. \tag{69}$$

At the same time, the error expression in Eq. (66) takes the diagrammatic form

$$\epsilon(t), \delta(t) \leq 1 - \frac{1}{2}\mathscr{L}^{-1}\,\mathrm{Tr}\left(Q\frac{1}{s-\mathcal{L}}\delta\rho_0\right) = 1 - \mathscr{L}^{-1}\langle\square\text{\textit{eee}}\rangle. \tag{70}$$

Using Dyson's expansion and the diagrammatic representation, we can now rewrite the term on the right as

$$\langle\square\text{\textit{eee}}\rangle = \langle\square\text{=}\rangle + \langle\square\text{=⊗=}\rangle + \langle\square\text{=⊗=⊗=}\rangle + \langle\square\text{=⊗=⊗=⊗=}\rangle + \ldots. \tag{71}$$

It can be further simplified once we take into account the fact that recovery dynamics preserves the states in the codespace, which means $\mathcal{L}_R\delta\rho_0 = 0$. Therefore,

$$\frac{1}{s-\kappa\mathcal{L}_R}\delta\rho_0 = \frac{1}{s}\delta\rho_0. \tag{72}$$

This property allows us to rewrite

$$\langle\square\text{\textit{eee}}\rangle = \frac{1}{s} + \frac{1}{s}\langle\square\text{=⊗}\rangle + \frac{1}{s}\langle\square\text{=⊗=⊗}\rangle + \frac{1}{s}\langle\square\text{=⊗=⊗=⊗}\rangle + \ldots. \tag{73}$$

Next, we use the decomposition

$$\exp(\kappa\mathcal{L}_R t) = \mathcal{W}_t + \left(1 - e^{-\kappa t}\right)\mathcal{R}, \tag{74}$$

25

where we defined $\mathcal{W}_t := e^{-\kappa t}\mathcal{K}_t$. In the space of imaginary frequencies, the same expression takes the form

$$\frac{1}{s - \kappa\mathcal{L}_R} = \mathcal{W}_s + \frac{\kappa}{s(s+\kappa)}\mathcal{R}, \qquad \mathcal{W}_s = \mathscr{L}\mathcal{W}_t. \tag{75}$$

This expression can also be written in diagrammatic form

$$== \longrightarrow + -, \qquad \frac{\kappa}{s(s+\kappa)}\mathcal{R} = \longrightarrow, \qquad \mathcal{W}_s = -. \tag{76}$$

Now let us consider the terms from the second to the ℓth (containing k operators $\mathcal{L}_E$, where $1 \leq k \leq \ell$), and rewrite each of them in the following form:

$$\left\langle \Box\!=\!\underbrace{\otimes\!=\!\otimes\ldots\otimes\!=\!\otimes}_{0 < k \leq \ell} \right\rangle = \left\langle \Box\!-\!\underbrace{\otimes\!-\!\otimes\ldots\otimes\!-\!\otimes}_{k} \right\rangle + \left\langle \Box\!\longrightarrow\!\underbrace{\otimes\!-\!\otimes\ldots\otimes\!-\!\otimes}_{k} \right\rangle$$
$$+ \left\langle \Box\!=\!\otimes\!\longrightarrow\!\underbrace{\otimes\!-\!\otimes\ldots\otimes\!-\!\otimes}_{k-1} \right\rangle + \cdots + \left\langle \Box\!=\!\underbrace{\otimes\!=\!\otimes\ldots\otimes\!=\!\otimes}_{k-1}\!\longrightarrow\!\otimes \right\rangle. \tag{77}$$

The right-hand side of this equation contains $k + 2$ terms. Our goal is to show that the right-hand side of this expression vanishes. We do so by using the following Lemma.

Lemma 2. *For any k satisfying $0 < k \leq \ell$ and any superoperator $\mathcal{O}$, we have* $\left\langle \mathcal{O}\!\longrightarrow\!\underbrace{\otimes\!-\!\otimes\ldots\otimes\!-\!\otimes}_{k} \right\rangle = 0$ *and* $\left\langle \mathcal{O}\!\longrightarrow\!-\!\underbrace{\otimes\!-\!\otimes\ldots\otimes\!-\!\otimes}_{k} \right\rangle = 0$.

Proof. To prove this statement, we first write the diagram in symbolic form:

$$\left\langle \mathcal{O}\!\longrightarrow\!\underbrace{\otimes\!-\!\otimes\ldots\otimes\!-\!\otimes}_{k} \right\rangle \equiv \frac{\Delta^k}{2}\mathrm{Tr}\left(\mathcal{O}\mathcal{R}\mathcal{L}_E(\mathcal{W}_s\mathcal{L}_E)^{k-1}\delta\rho_0\right),$$
$$\left\langle \mathcal{O}\!\longrightarrow\!-\!\underbrace{\otimes\!-\!\otimes\ldots\otimes\!-\!\otimes}_{k} \right\rangle \equiv \frac{\Delta^k}{2}\mathrm{Tr}\left(\mathcal{O}\mathcal{R}\mathcal{W}_s\mathcal{L}_E(\mathcal{W}_s\mathcal{L}_E)^{k-1}\delta\rho_0\right). \tag{78}$$

Next, we express the action of the Lindblad generators in a more explicit form:

$$\mathcal{L}_E(\mathcal{W}_s\mathcal{L}_E)^{k-1}\rho = \sum_{\boldsymbol{\mu},\boldsymbol{\mu}'\in M_C} a_{\boldsymbol{\mu}\boldsymbol{\mu}'}K_{\boldsymbol{\mu}}\rho K_{\boldsymbol{\mu}'}^\dagger,$$
$$\mathcal{W}_s\mathcal{L}_E(\mathcal{W}_s\mathcal{L}_E)^{k-1}\rho = \sum_{\boldsymbol{\mu},\boldsymbol{\mu}'\in M_C} b_{\boldsymbol{\mu}\boldsymbol{\mu}'}K_{\boldsymbol{\mu}}\rho K_{\boldsymbol{\mu}'}^\dagger, \tag{79}$$

where M_C is the set of all correctable error sequences, and $a_{\boldsymbol{\mu}\boldsymbol{\mu}'}$, $b_{\boldsymbol{\mu}\boldsymbol{\mu}'}$ are certain real numbers, and we used the fact that $\mathcal{W}_s$ does not increase the number of errors. It is important to note that, as the action of any Linbladian operator must return traceless operators and the map $\mathcal{W}_s$ preserves the trace, these operators must satisfy

$$\forall \rho, k > 0: \quad \mathrm{Tr}\left(\mathcal{L}_E(\mathcal{W}_s\mathcal{L}_E)^{k-1}\rho\right) = 0, \quad \mathrm{Tr}\left(\mathcal{W}_s\mathcal{L}_E(\mathcal{W}_s\mathcal{L}_E)^{k-1}\rho\right) = 0. \tag{80}$$

For any ρ, these conditions are satisfied if and only if

$$\sum_{\boldsymbol{\mu},\boldsymbol{\mu}'\in M_C} a_{\boldsymbol{\mu}\boldsymbol{\mu}'} K_{\boldsymbol{\mu}'}^\dagger K_{\boldsymbol{\mu}} = 0, \qquad \sum_{\boldsymbol{\mu},\boldsymbol{\mu}'\in M_C} b_{\boldsymbol{\mu}\boldsymbol{\mu}'} K_{\boldsymbol{\mu}'}^\dagger K_{\boldsymbol{\mu}} = 0. \tag{81}$$

Now we can express the portion of the expression inside the trace in Eq. (78) using the property of the recovery operator in Eq. (59):

$$\begin{aligned}
\mathcal{R}\mathcal{L}_E(\mathcal{W}_s\mathcal{L}_E)^{k-1}\delta\rho_0 &= \sum_{\boldsymbol{\mu},\boldsymbol{\mu}'\in M_C} a_{\boldsymbol{\mu}\boldsymbol{\mu}'}\mathcal{R}(K_{\boldsymbol{\mu}}\delta\rho_0 K_{\boldsymbol{\mu}'}^\dagger) \\
&= \delta\rho_0 \sum_{\boldsymbol{\mu},\boldsymbol{\mu}'\in M_C} a_{\boldsymbol{\mu}\boldsymbol{\mu}'} C_{\boldsymbol{\mu}'\boldsymbol{\mu}} = \delta\rho_0 \sum_{\boldsymbol{\mu},\boldsymbol{\mu}'\in M_C} a_{\boldsymbol{\mu}\boldsymbol{\mu}'}\langle 0|K_{\boldsymbol{\mu}'}^\dagger K_{\boldsymbol{\mu}}|0\rangle = 0.
\end{aligned} \tag{82}$$

Similarly,

$$\begin{aligned}
\mathcal{R}\mathcal{W}_s\mathcal{L}_E(\mathcal{W}_s\mathcal{L}_E)^{k-1}\delta\rho_0 &= \sum_{\boldsymbol{\mu},\boldsymbol{\mu}'\in M_C} b_{\boldsymbol{\mu}\boldsymbol{\mu}'}\mathcal{R}(K_{\boldsymbol{\mu}}\delta\rho_0 K_{\boldsymbol{\mu}'}^\dagger) \\
&= \delta\rho_0 \sum_{\boldsymbol{\mu},\boldsymbol{\mu}'\in M_C} b_{\boldsymbol{\mu}\boldsymbol{\mu}'} C_{\boldsymbol{\mu}'\boldsymbol{\mu}} = \delta\rho_0 \sum_{\boldsymbol{\mu},\boldsymbol{\mu}'\in M_C} b_{\boldsymbol{\mu}\boldsymbol{\mu}'}\langle 0|K_{\boldsymbol{\mu}'}^\dagger K_{\boldsymbol{\mu}}|0\rangle = 0.
\end{aligned} \tag{83}$$

Thus, both expressions in Eq. (78) vanish and this leads to the statement of the Lemma.

As a result of this Lemma, all terms on the right-hand side of Eq. (77) vanish immediately. To show that the first term must vanish, we can use the definition of the operator Q below Eq. (64) and rewrite

$$\langle \square\!\!-\!\!\otimes^k \rangle = \langle (\delta\rho_0 \otimes I)\!\!\rightarrow\!\!-\!\!\underbrace{\otimes\!\!-\!\!\otimes\ldots\otimes\!\!-\!\!\otimes}_{k} \rangle. \tag{84}$$

Therefore we have

$$\langle \square\!\!=\!\!\underbrace{\otimes\!\!=\!\!\otimes\ldots\otimes\!\!=\!\!\otimes}_{0 < k \le \ell} \rangle = 0. \tag{85}$$

Following the removal of the vanishing terms, we obtain the series

$$\langle \square\!\ell\ell\ell \rangle = \frac{1}{s} + \frac{1}{s}\langle \square\!\!=\!\!\underbrace{\otimes\!\!=\!\!\otimes\ldots\otimes\!\!=\!\!\otimes}_{\ell+1} \rangle + \frac{1}{s}\langle \square\!\!=\!\!\underbrace{\otimes\!\!=\!\!\otimes\ldots\otimes\!\!=\!\!\otimes}_{\ell+2} \rangle + \frac{1}{s}\langle \square\!\!=\!\!\underbrace{\otimes\!\!=\!\!\otimes\ldots\otimes\!\!=\!\!\otimes}_{\ell+3} \rangle + \ldots. \tag{86}$$

This expression can be compacted again using Eq. (69) to obtain

$$\langle \square\!\ell\ell\ell \rangle = \frac{1}{s} + \frac{1}{s}\langle \square\!\ell\ell\ell\underbrace{\otimes\!\!=\!\!\otimes\ldots\otimes\!\!=\!\!\otimes}_{\ell+1} \rangle. \tag{87}$$

The rest of the proof uses this expression iteratively. As the first step, we rewrite Eq. (87) as

$$\langle \square\!\ell\ell\ell \rangle = \frac{1}{s} + \frac{1}{s}\langle \square\!\ell\ell\ell\underbrace{\otimes\!\!=\!\!\otimes\ldots\otimes\!\!=\!\!\otimes}_{\ell}\!\!-\!\!\otimes \rangle + \frac{1}{s}\langle \square\!\ell\ell\ell\underbrace{\otimes\!\!=\!\!\otimes\ldots\otimes\!\!=\!\!\otimes}_{\ell}\!\!\rightarrow\!\!\otimes \rangle. \tag{88}$$

27

The last term vanishes as a result of Lemma 2, and, as a second step, we rewrite the remaining terms as

$$\left\langle \square \text{⬛⬛⬛} \right\rangle = \frac{1}{s} + \frac{1}{s}\left\langle \square \text{⬛⬛⬛} \underbrace{\otimes\!\!=\cdots=\!\!\otimes}_{\ell}\!-\!\otimes \right\rangle = \frac{1}{s} + \frac{1}{s}\left\langle \square \text{⬛⬛⬛} \underbrace{\otimes\!\!=\cdots=\!\!\otimes}_{\ell}\!-\!\otimes \right\rangle. \tag{89}$$

We repeat these two steps $\ell - 1$ more times to get

$$\left\langle \square \text{⬛⬛⬛} \right\rangle = \frac{1}{s} + \frac{1}{s}\left\langle \square \text{⬛⬛⬛} \underbrace{\otimes\!\!-\!\!\otimes\cdots\otimes\!\!-\!\!\otimes}_{\ell+1} \right\rangle. \tag{90}$$

We can derive a bound on the last term of this expression using

$$\mathscr{L}^{-1}\frac{1}{s}\left\langle \square \text{⬛⬛⬛} \underbrace{\otimes\!\!-\!\!\otimes\cdots\otimes\!\!-\!\!\otimes}_{\ell+1} \right\rangle = \frac{\Delta^{\ell+1}}{2}\mathcal{T}\int dt_1 \ldots dt_{\ell+2}\mathrm{Tr}\left(Q e^{\mathcal{L}(t_2-t_1)}\mathcal{L}_E\mathcal{W}_{t_3-t_2}\ldots\mathcal{W}_{t_{\ell+2}-t_{\ell+1}}\mathcal{L}_E\delta\rho_0 \right)$$

$$\geq -(\|\mathcal{L}_E\|_\mathsf{K}\Delta)^{\ell+1}\mathcal{T}\int dt_1 \ldots dt_{\ell+2}\|e^{\mathcal{L}(t_2-t_1)}\|\|\mathcal{W}_{t_3-t_2}\|\ldots\|\mathcal{W}_{t_{\ell+2}-t_{\ell+1}}\|$$

$$= -(\|\mathcal{L}_E\|_\mathsf{K}\Delta)^{\ell+1}\mathscr{L}^{-1}\left\{ \frac{1}{s^2(s+\kappa)^\ell} \right\}, \tag{91}$$

where we defined the time-ordered exponential as

$$\mathcal{T}\int dt_1 \ldots dt_k = \int_0^t dt_1 \int_0^{t_1} dt_2 \cdots \int_0^{t_{k-1}} dt_k, \tag{92}$$

used that the spectral norms of the operators and superoperators yield

$$\|Q\| = 1, \qquad \|e^{\mathcal{L}t}\| = 1, \qquad \|\mathcal{W}_t\| = e^{-\kappa t}\|\mathcal{K}_t\| = e^{-\kappa t}. \tag{93}$$

Therefore, we arrive at the expression

$$\mathscr{L}^{-1}\left\langle \square \text{⬛⬛⬛} \right\rangle \geq 1 - (\|\mathcal{L}_E\|_\mathsf{K}\Delta)^{\ell+1}\mathscr{L}^{-1}\left\{ \frac{1}{s^2(s+\kappa)^\ell} \right\}. \tag{94}$$

Performing inverse Fourier transform, we finally get

$$\epsilon(t), \delta(t) \leq 1 - \mathscr{L}^{-1}\left\langle \square \text{⬛⬛⬛} \right\rangle \leq \left(\frac{\|\mathcal{L}_E\|_\mathsf{K}\Delta}{\kappa} \right)^{\ell+1} F\left(\kappa t\right). \tag{95}$$

This expression concludes our proof.

Appendix C: Proof of Lemma 1

This appendix contains the proof of Lemma 1. To express the logical error, we first consider the trajectory decomposition in Eq. (16). This allows us to derive the bound

$$\epsilon(t) = 1 - \min_{\rho_0}\sum_{\boldsymbol{\mu}\in F} p(\boldsymbol{\mu}, t)\mathrm{Tr}\left(\rho_0\mathcal{R}\mathcal{E}_{\boldsymbol{\mu}}\rho_0\right)$$

$$= \max_{\rho_0}\sum_{\boldsymbol{\mu}\in F} p(\boldsymbol{\mu}, t)\left(1 - \mathrm{Tr}\left(\rho_0\mathcal{R}\mathcal{E}_{\boldsymbol{\mu}}\rho_0\right)\right) \leq \max_{\rho_0}\sum_{\boldsymbol{\mu}\in F} p(\boldsymbol{\mu}, t)\Theta\left(1 - \mathrm{Tr}\left(\rho_0\mathcal{R}\mathcal{E}_{\boldsymbol{\mu}}\rho_0\right)\right), \tag{96}$$

where the minimization/maximization is over pure states ρ_0 in the codespace C, and $\Theta(x)$ is the Heaviside step function (defined as $\Theta(x) = 0$ for $x < 0$ and $\Theta(x) = 1$ for $x \geq 0$). We also used the property that $\Theta(x) \geq x$ for $x \in [0, 1]$.

Next, we use the definition of faithful trajectory $\boldsymbol{\mu} \in G$ and express

$$\forall \boldsymbol{\mu} \in G: \quad \mathcal{R}\mathcal{E}_{\boldsymbol{\mu}}\rho_0 = \mathcal{R}\mathcal{E}_{\boldsymbol{\mu}}\mathcal{R}\rho_0 = \left(\prod_m (\mathcal{R}\mathcal{E}_{\boldsymbol{\mu}_m}\mathcal{R}) \right) \rho_0, \tag{97}$$

where $\boldsymbol{\mu}_m$ are error subsequences. For any state ρ, we have

$$\mathcal{R}\mathcal{E}_{\boldsymbol{\mu}_m}\mathcal{R}(\rho) = \mathcal{R}(E_{\boldsymbol{\mu}_m}\mathcal{R}(\rho)E_{\boldsymbol{\mu}_m}^\dagger) = C_{\boldsymbol{\mu}_m\boldsymbol{\mu}_m}\mathcal{R}(\rho) = \langle 0|E_{\boldsymbol{\mu}_m}^\dagger E_{\boldsymbol{\mu}_m}|0\rangle\mathcal{R}(\rho) = \mathcal{R}(\rho), \tag{98}$$

where we used Eq. (59) and the fact that the sequence $\boldsymbol{\mu}_m$ has weight smaller than the radius ℓ and, thus, satisfies Knill-Laflamme condition. Thus, for any faithful trajectory we have

$$\mathcal{R}\mathcal{E}_{\boldsymbol{\mu}}\rho_0 = \mathcal{R}(\rho_0) = \rho_0. \tag{99}$$

Finally, using the fact that extremum over ρ_0 is taken over a pure states, we get

$$\forall \boldsymbol{\mu} \in G: \quad \mathrm{Tr}\left(\rho_0\mathcal{R}\mathcal{E}_{\boldsymbol{\mu}}\rho_0\right) = \mathrm{Tr}\,\rho_0^2 = 1. \tag{100}$$

Combining this expression and the definition of the Heaviside function, we find from Eq. (96) that

$$\epsilon(t) \leq \max_{\rho_0} \sum_{\boldsymbol{\mu} \in F\backslash G} p(\boldsymbol{\mu}, t)\Theta\left(1 - \mathrm{Tr}\left(\rho_0\mathcal{E}_{\boldsymbol{\mu}}\rho_0\right)\right) + \max_{\rho_0} \sum_{\boldsymbol{\mu} \in G} p(\boldsymbol{\mu}, t)\Theta\left(1 - \mathrm{Tr}\left(\rho_0\mathcal{E}_{\boldsymbol{\mu}}\rho_0\right)\right). \tag{101}$$

The last term vanishes due to Eq. (100). Taking into account the fact that $\Theta(x) \leq 1$, we get

$$\epsilon(t) \leq \sum_{\boldsymbol{\mu} \in F\backslash G} p(\boldsymbol{\mu}, t). \tag{102}$$

This concludes our proof.

Appendix D: Proof of Theorem 2

This appendix contains the definition of the threshold and the proof of Theorem 2. For the purposes of this appendix, we adopt the following definition of the threshold for an n-qubit quantum error-correcting code:

Definition 2. *Consider a family of n-qubit error-correcting codes for increasing n. Each code has a codespace C, code distance $d = d(n)$, an error channel $\mathcal{E}$ and a recovery map $\mathcal{R}$. We say that the code family has a tolerable error weight h if $h = h(n)$ is an integer-valued function such that, for any $|\psi\rangle \in \mathsf{C}$ and non-negative integer $k \leq h$, the following inequality holds:*

$$\mathcal{R}\mathcal{E}^k\left(|\psi\rangle\langle\psi|\right) - (1 - \xi)|\psi\rangle\langle\psi| \geq 0, \tag{103}$$

where $\xi = 2^{-\Omega(d)}$ is independent of $|\psi\rangle$. Let G be the set of all possible constants f such that $h(n) = \lfloor fn \rfloor$ is a tolerable error weight. We say that the code family has a threshold f_c if $f_c = \sup G > 0$.

The inequality in Eq. (103) means that the eigenvalues of the operator on the left side of the inequality are non-negative. Since $\mathcal{R}\mathcal{E}^k$ is a quantum channel, this inequality is equivalent to the statement $\mathcal{R}\mathcal{E}^k|\psi\rangle\langle\psi| = (1-\xi)|\psi\rangle\langle\psi| + \sum_i p_i|\psi_i\rangle\langle\psi_i|$ for some $|\psi_i\rangle \in \mathsf{C}$ and $p_i \geq 0$ that satisfy $\sum_i p_i \leq \xi$. In other words, for any initial logical state, the error occurs with ξ-small probability. By this definition, an n-qubit code with a threshold can recover the encoded quantum information with arbitrary precision, even if it is subjected to a large number of $k \leq h$ error channel rounds. Examples of error-correcting codes that can withstand uniform single-qubit Pauli noise include the repetition code and many quantum stabilizer codes such as the toric code and color codes.

Recall that, for a Poissonian noise channel, the error jump operators satisfy $\sum_{\mu=1}^N E_\mu^\dagger E_\mu = NI$. The Lindbladian can be written in a similar form as Eq. (16)

$$\mathcal{L}\rho = \frac{d}{dt}\rho = \kappa\left(\mathcal{R}(\rho) - \rho\right) + \Delta\sum_{\mu=1}^N\left(E_\mu\rho E_\mu^\dagger - \frac{1}{2}E_\mu^\dagger E_\mu\rho - \frac{1}{2}\rho E_\mu^\dagger E_\mu\right)$$
$$= (\kappa + N\Delta)\left(p_0\left(\mathcal{E}_0(\rho) - \rho\right) + p_1\left(\mathcal{E}_1(\rho) - \rho\right)\right), \tag{104}$$

where the recovery $\mathcal{E}_0 = \mathcal{R}$ and the error process $\mathcal{E}_1(\cdot) = \frac{1}{N}\sum_\mu E_\mu(\cdot)E_\mu^\dagger$ have probabilities $p_0 = \frac{\kappa}{\kappa+N\Delta}$ and $p_1 = \frac{N\Delta}{\kappa+N\Delta}$, respectively. Using a Taylor expansion, we get

$$\exp(\mathcal{L}t) = e^{-(\kappa+N\Delta)t}\exp\left((\kappa+N\Delta)t\sum_{\mu\in\{0,1\}}p_\mu\mathcal{E}_\mu\right) = \sum_{k=0}^\infty \mathcal{P}(k)\frac{(t(\kappa+N\Delta))^k}{k!}e^{-t(\kappa+N\Delta)}, \tag{105}$$

where the channel $\mathcal{P}(k)$ is defined as $\mathcal{P}(k) = (p_0\mathcal{E}_0 + p_1\mathcal{E}_1)^k = \sum_{\{\mathbf{a}\}}p_{a_1}p_{a_2}\cdots p_{a_k}\mathcal{E}_{a_1}\mathcal{E}_{a_2}\cdots\mathcal{E}_{a_k}$ and $\{\mathbf{a}\}$ is a set of all possible binary (jump) sequences of length k with $a_i \in \{0,1\}$ labeling the recovery and error channels. This is an alternative form of Eq. (16). Using the definition of the error measure $\epsilon(t)$ [Eq. (11)], we find that, for an initial pure state ρ_0 in the codespace, we have

$$\epsilon(t) = \sum_{k=0}^\infty p_e(k)\frac{(t(\kappa+N\Delta))^k}{k!}e^{-t(\kappa+N\Delta)}, \tag{106}$$

where $p_e(k) = 1 - \min_{\rho_0}\sum_{\{\mathbf{a}\}}p_{a_1}p_{a_2}\cdots p_{a_k}\mathrm{Tr}\left[\rho_0\mathcal{R}\mathcal{E}_{a_1}\mathcal{E}_{a_2}\cdots\mathcal{E}_{a_k}\rho_0\right]$. For integers $k \geq 1, h \geq 1$, a sequence $\mathbf{a} = (a_1,\ldots,a_k)$ has an error weight of at most h if it contains no more than h consecutive error jumps. Let $\{\mathbf{a}_h\}$ be the set of all jump sequences of length k with an error weight of at most h. Since $\{\mathbf{a}_h\} \subseteq \{\mathbf{a}\}$, it follows that

$$\min_{\rho_0}\sum_{\{\mathbf{a}_h\}}p_{a_1}p_{a_2}\cdots p_{a_k}\mathrm{Tr}\left[\rho_0\mathcal{R}\mathcal{E}_{a_1}\mathcal{E}_{a_2}\cdots\mathcal{E}_{a_k}\rho_0\right] \leq \min_{\rho_0}\sum_{\{\mathbf{a}\}}p_{a_1}p_{a_2}\cdots p_{a_k}\mathrm{Tr}\left[\rho_0\mathcal{R}\mathcal{E}_{a_1}\mathcal{E}_{a_2}\cdots\mathcal{E}_{a_k}\rho_0\right]. \tag{107}$$

To establish an upper bound on $\epsilon(t)$, let h be a tolerable error weight for the code satisfying Eq. (103). Let $z \geq 0$ denote the number of zeros in the sequence $\mathbf{a}_h = (a_1, a_2, \cdots, a_k)$. Then

$$\mathcal{E}_{a_1}\mathcal{E}_{a_2}\cdots\mathcal{E}_{a_k} = \mathcal{E}_1^{m_0}\mathcal{R}\mathcal{E}_1^{m_1}\cdots\mathcal{R}\mathcal{E}_1^{m_z}, \tag{108}$$

where $0 \leq m_i \leq h$ for $i = 0,\ldots,z$ and $z + \sum_{i=0}^z m_i = k$. Let us rewrite

$$\mathrm{Tr}\left[\rho_0\mathcal{R}\mathcal{E}_1^{m_0}\cdots\mathcal{R}\mathcal{E}_1^{m_{z-1}}\mathcal{R}\mathcal{E}_1^{m_z}\rho_0\right] = \mathrm{Tr}\left[\rho_0\mathcal{R}\mathcal{E}_1^{m_0}\cdots\mathcal{R}\mathcal{E}_1^{m_{z-1}}\left(\mathcal{R}\mathcal{E}_1^{m_z}\rho_0 - (1-\xi)\rho_0\right)\right]$$
$$+ (1-\xi)\mathrm{Tr}\left[\rho_0\mathcal{R}\mathcal{E}_1^{m_0}\cdots\mathcal{R}\mathcal{E}_1^{m_{z-1}}\rho_0\right]. \tag{109}$$

By the definition of threshold, it follows from Eq. (103) that the first term on the right-hand side of Eq. (109) is non-negative. Therefore, if $m_z > 0$, then

$$\text{Tr}\left[\rho_0 \mathcal{R}\mathcal{E}_1^{m_0} \cdots \mathcal{R}\mathcal{E}_1^{m_{z-1}} \mathcal{R}\mathcal{E}_1^{m_z} \rho_0\right] \geq (1 - \xi)\text{Tr}\left[\rho_0 \mathcal{R}\mathcal{E}_1^{m_0} \cdots \mathcal{R}\mathcal{E}_1^{m_{z-1}} \rho_0\right]. \tag{110}$$

If $m_z = 0$, we have instead

$$\text{Tr}\left[\rho_0 \mathcal{R}\mathcal{E}_1^{m_0} \cdots \mathcal{R}\mathcal{E}_1^{m_{z-1}} \mathcal{R}\mathcal{E}_1^{m_z} \rho_0\right] = \text{Tr}\left[\rho_0 \mathcal{R}\mathcal{E}_1^{m_0} \cdots \mathcal{R}\mathcal{E}_1^{m_{z-1}} \rho_0\right]. \tag{111}$$

Inductively, we know that after $z + 1$ steps, the exponent of the factor $(1 - \xi)$ will be equal to the number of non-zero m_i's in the jump sequence. We therefore find that

$$\text{Tr}\left[\rho_0 \mathcal{R}\mathcal{E}_1^{m_0} \cdots \mathcal{R}\mathcal{E}_1^{m_{z-1}} \mathcal{R}\mathcal{E}_1^{m_z} \rho_0\right] \geq (1 - \xi)^{(k+1)/2} \geq (1 - \xi)^k, \tag{112}$$

where we obtained an upper bound on the number of non-zero m_i's by setting $m_i = 1$ for all i in the relation $z + \sum_{i=0}^{z} m_i = k$. The number of non-zero m_i's is thus less than or equal to $(k + 1)/2$.

Now we are ready to prove the following Lemma:

Lemma 3. *Assume an n-qubit code family with increasing n and a tolerable error weight $h = h(n)$ with respect to the error channel $\mathcal{E}(\cdot) = \frac{1}{N} \sum_\mu E_\mu(\cdot) E_\mu^\dagger$. Then there exists $\xi = 2^{-\Omega(d)}$ such that*

$$p_e(k) \leq 1 - \left[(1 - \xi)\left(1 - p_1^{h+1}\right)\right]^k, \tag{113}$$

where $p_1 = \frac{N\Delta}{\kappa + N\Delta}$ and $k \geq 0$.

Proof. The equality trivially holds for $k = 0$. We therefore consider the case $k \geq 1$. To establish an upper bound on this probability, we use Eq. (107) and Eq. (112) to obtain

$$p_e(k) \leq 1 - \min_{\rho_0} \sum_{\{\mathbf{a}_h\}} p_{a_1} p_{a_2} \cdots p_{a_k} \text{Tr}\left[\rho_0 \mathcal{R}\mathcal{E}_{a_1} \mathcal{E}_{a_2} \cdots \mathcal{E}_{a_k} \rho_0\right] \leq 1 - (1 - \xi)^k \sum_{\{\mathbf{a}_h\}} p_{a_1} p_{a_2} \cdots p_{a_k}. \tag{114}$$

We want to show that

$$\left(1 - p_1^{h+1}\right)^k \leq \sum_{\{\mathbf{a}_h\}} p_{a_1} p_{a_2} \cdots p_{a_k}. \tag{115}$$

To show this, we note that, for a given jump sequence $\mathbf{a}_h$, its probability in Eq. (115) takes the form

$$p_{a_1} p_{a_2} \cdots p_{a_k} = p_1^{m_0} p_0 p_1^{m_2} p_0 \cdots p_1^{m_z}, \tag{116}$$

where $z + \sum_{i=0}^{z} m_i = k$ and each integer satisfies $0 \leq m_i \leq h$. Each jump sequence $\mathbf{a}_h$ is uniquely labelled by $\mathbf{m}(\mathbf{a}_h) = (m_0, m_1, \cdots, m_z)$. We can establish the desired lower bound

by noting that, when $p_0 \neq 0$,

$$
\begin{aligned}
(1 - p_1^{h+1})^k &= \left[\sum_{i=0}^{h} p_1^i p_0 \right]^k = \sum_{i_1=0}^{h} \sum_{i_2=0}^{h} \cdots \sum_{i_k=0}^{h} p_1^{i_1} p_0 p_1^{i_2} p_0 \cdots p_1^{i_k} p_0 \\
&= \sum_{z=0}^{k} \sum_{\mathbf{m}} \underbrace{p_1^{m_0} p_0 p_1^{m_1} p_0 \cdots p_1^{m_z}}_{\text{first } k \text{ factors}} \times \left[\sum_{i'=0}^{h-m_z} p_1^{i'} p_0 \right] \times \left[\sum_{i=0}^{h} p_1^i p_0 \right]^{k-z-1} \\
&\leq \sum_{z=0}^{k} \sum_{\mathbf{m}} p_1^{m_1} p_0 p_1^{m_2} p_0 \cdots p_1^{m_z} \\
&= \sum_{\{\mathbf{a}_h\}} p_{a_1} p_{a_2} \cdots p_{a_k}.
\end{aligned}
\tag{117}
$$

In the second line, the sum is over $\mathbf{m} = (m_0, m_1, \cdots, m_z)$, where $0 \leq m_i \leq h$ and $z + \sum_{i=0}^{z} m_i = k$. In going from the first line to the second line, we re-write the sum in the first line using the following steps: we fix the first k factors in each term and sum over the rest of the possible factors. Then we take the sum over all possible first k factors (i.e. $\sum_{z=0}^{k} \sum_{\mathbf{m}}$). The inequality in the third line follows from $\left[\sum_{i'=0}^{h-m_z} p_1^{i'} p_0 \right] \left[\sum_{i=0}^{h} p_1^i p_0 \right]^{k-z-1} \leq 1$, which trivially holds for $z \leq k - 1$. When $z = k$ and $p_0 \neq 0$, we have $m_i = 0$ for all i due to the constraint $z + \sum_{i=0}^{z} m_i = k$. Therefore, the two factors cancel, and the inequality becomes an equality. When $p_0 = 0$, we can directly verify that Eq. (117) also holds. This concludes the proof of the lemma.

$\square$

If we substitute Eq. (113) into Eq. (106), we get

$$
\begin{aligned}
\epsilon(t) &= \sum_{k} p_e(k) \frac{[t(\kappa + N\Delta)]^k}{k!} e^{-t(\kappa + N\Delta)} \\
&\leq \sum_{k} \left(1 - \left[(1 - \xi) \left(1 - \left(\frac{N\Delta}{\kappa + N\Delta} \right)^{h+1} \right) \right]^k \right) \frac{[t(\kappa + N\Delta)]^k}{k!} e^{-t(\kappa + N\Delta)} \\
&= 1 - \exp\left(-(1 - \xi)(\kappa + N\Delta) \left(\frac{N\Delta}{\kappa + N\Delta} \right)^{h+1} t - \xi(\kappa + N\Delta)t \right) \\
&= 1 - \exp\left(-N\Delta(1 - \xi) \left(\frac{N\Delta}{\kappa + N\Delta} \right)^{h} t - \xi(\kappa + N\Delta)t \right),
\end{aligned}
\tag{118}
$$

which proves Theorem 2.

We would like to conclude this Appendix with a side remark on the definition of the tolerable error weight and the threshold. In Definition 2, instead of Eq. (103), we can also consider a natural alternative condition on the measure of fidelity:

$$
\text{Tr}\left[\rho \mathcal{R} \mathcal{E}^m \rho \right] \geq 1 - \xi, \qquad \rho = |\psi\rangle\langle\psi|,
\tag{119}
$$

for $\xi \in [0,1]$ and $0 \le m \le h$. This condition is necessary but not sufficient for Eq. (103) to hold. For instance, a pure logical state $|\psi'\rangle$ with a small logical rotation from the original logical state $|\psi\rangle$ can satisfy Eq. (119) but will fail to satisfy Eq. (103). Note that $\mathrm{Tr}\,[\rho \mathcal{RE}^m \rho] = F(\rho, \mathcal{RE}^m \rho)^2$, where the fidelity between two quantum states ρ, σ is defined as $F(\rho, \sigma) = \mathrm{Tr}\,(\sqrt{\rho^{1/2} \sigma \rho^{1/2}})$. For any quantum state γ, we have [69]

$$F(\rho, \sigma) \ge F(\rho, \gamma) F(\gamma, \sigma) - \sqrt{1 - F(\rho, \gamma)^2} \sqrt{1 - F(\gamma, \sigma)^2}. \tag{120}$$

The fidelity measure also satisfies joint concavity [69]

$$F\left(\sum_i p_i \rho_i, \sum_i p_i \sigma_i\right) \ge \sum_i p_i F(\rho_i, \sigma_i), \tag{121}$$

where p_i's form a probability distribution over quantum states ρ_i, σ_i. For a generic mixed state in the codespace $\rho = \alpha |\psi\rangle\langle\psi| + (1-\alpha)|\phi\rangle\langle\phi|$, with $\alpha \in [0,1]$ and $|\psi\rangle, |\phi\rangle \in \mathsf{C}$, it follows from the joint concavity that

$$F(\rho, \mathcal{RE}_1^m \rho) \ge \alpha F(\rho_\psi, \mathcal{RE}_1^m \rho_\psi) + (1-\alpha) F(\rho_\phi, \mathcal{RE}_1^m \rho_\phi) \ge \sqrt{1-\xi}, \tag{122}$$

where $\rho_\psi = |\psi\rangle\langle\psi|$ and $\rho_\phi = |\phi\rangle\langle\phi|$. The last line follows once the integer m satisfies $0 \le m \le h$. For convenience, let us denote $\mathcal{M}_z = \prod_{i=0}^z \mathcal{RE}_1^{m_i}$. Using inequality (120) and the fact that $\sqrt{1 - F(\rho_0, \mathcal{M}_z \rho_0)^2} \le 1$, we can deduce that, if $m_z > 0$,

$$F(\rho_0, \mathcal{M}_z \rho_0) \ge F(\rho_0, \mathcal{M}_{z-1}\rho_0) F(\mathcal{M}_{z-1}\rho_0, \mathcal{M}_z \rho_0) - \sqrt{1 - F(\mathcal{M}_{z-1}\rho_0, \mathcal{M}_z \rho_0)^2}$$
$$\ge \sqrt{1-\xi} F(\rho_0, \mathcal{M}_{z-1}\rho_0) - \sqrt{\xi}, \tag{123}$$

where the last line follows from $F(\mathcal{M}_{z-1}\rho_0, \mathcal{M}_z \rho_0) \ge \sqrt{1-\xi}$ when setting $\rho = \mathcal{M}_{z-1}\rho_0$ in Eq. (122). We also have $F(\rho_0, \mathcal{M}_z \rho_0) = F(\rho_0, \mathcal{M}_{z-1}\rho_0)$ if $m_z = 0$. From Eq. (123), we note that

$$\sqrt{1-\xi} F(\rho_0, \mathcal{M}_{z-1}\rho_0) - \sqrt{\xi} \ge \sqrt{1 - \xi^{1/4}} F(\rho_0, \mathcal{M}_{z-1}\rho_0) - \sqrt{\xi} \tag{124}$$

for $0 \le \xi \le 1$. Applying the inequality inductively, similarly to the inductive derivation of Eq. (112), we have

$$F(\rho_0, \mathcal{M}_z \rho_0) \ge \left(1 - \xi^{1/4}\right)^{k/2} - \sqrt{\xi}\, \frac{1 - \left(1 - \xi^{1/4}\right)^{k/2}}{1 - \sqrt{1 - \xi^{1/4}}} \ge \left(1 - \xi^{1/4}\right)^{k/2} - 2\xi^{1/4}. \tag{125}$$

The second inequality follows from the use of Bernoulli's inequality $\sqrt{1 - \xi^{1/4}} \le 1 + \xi^{1/4}/2$. Since $F(\rho_0, \mathcal{M}_z \rho_0) \ge 0$, this implies

$$F(\rho_0, \mathcal{M}_z \rho_0)^2 \ge \left(1 - \xi^{1/4}\right)^k - 4\xi^{1/4}. \tag{126}$$

To bound Eq. (106), we note that

$$p_e(k) = 1 - \min_{\rho_0} \sum_{\{\mathbf{a}\}} p_{a_1} p_{a_2} \cdots p_{a_k} \text{Tr}\left[\rho_0 \mathcal{R} \mathcal{E}_{a_1} \mathcal{E}_{a_2} \cdots \mathcal{E}_{a_k} \rho_0\right]$$

$$= 1 - \min_{\rho_0} \sum_{\{\mathbf{a}\}} p_{a_1} p_{a_2} \cdots p_{a_k} F(\rho_0, \mathcal{M}_z \rho_0)^2$$

$$\leq 1 + 4\xi^{1/4} - \left(1 - \xi^{1/4}\right)^k \sum_{\{\mathbf{a}\}} p_{a_1} p_{a_2} \cdots p_{a_k}$$

$$\leq 1 + 4\xi^{1/4} - \left(1 - \xi^{1/4}\right)^k \left(1 - p_1^{h+1}\right)^k, \tag{127}$$

where z denotes the number of 0's in the jump sequence $\mathbf{a}$, and we used Eq. (115) in the last line. Substituting this into Eq. (106), we get a modified Theorem 2 based on this alternative definition of the tolerable error weight and the threshold:

$$\epsilon(t) \leq 1 + 4\xi^{1/4} - \exp\left(-N\Delta(1 - \xi^{1/4})\left(\frac{N\Delta}{\kappa + N\Delta}\right)^h t - \xi^{1/4}(\kappa + N\Delta)t\right). \tag{128}$$

Note that ξ, and hence the contribution $\xi^{1/4}$, is exponentially small in the distance of the quantum codes. For codes with a large enough distance, the bound yields qualitatively the same scaling of the error rate as Eq. (118) as the code distance increases.

Appendix E: Proof of Theorem 3

This appendix contains the necessary assumptions and the proof of Theorem 3. In particular, we consider a noise model where the error jump operators satisfy $E_\mu^2 = I$ and $E_\mu E_{\mu'} = \pm E_{\mu'} E_\mu$ for all μ, μ'. This noise model is a special case of a Poisonnian noise model. We will assume exactly the same setup as in the previous appendix, i.e. Eqs. (104) and (106). We prove an error bound for the class of n-qubit error-correcting codes C that have a varying distance $d = d(n)$ and a tolerable error weight $h(n)$ tailored for this particular noise model (see Eq. (130) for a precise definition).

An error configuration is a state $E_{\{\mu\}}|\psi\rangle\langle\psi|E_{\{\mu\}}^\dagger$ for some fixed reference state $|\psi\rangle \in \mathsf{C}$, where the operator $E_{\{\mu\}} = \prod_{\mu \in \{\mu\}} E_\mu$ is the error operator that creates the configuration and $\{\mu\}$ is a subset of (distinct) error indices that indicate the errors contained in the configuration (see Eq. (3)). The size of the set $\{\mu\}$ is the number of physical errors in the error configuration. For convenience, we define $\mathcal{Q}_k$ to be the error channel that creates a mixture of error configurations containing k physical errors and is symmetric under any relabeling (permutation) of the error indices μ. More precisely, we define $\mathcal{Q}_0 = \mathcal{I}$ to be the identity channel. For $k \geq 1$, we define $\mathcal{Q}_k(\cdot) = \frac{1}{|\mathbf{S}_k|} \sum_{\{\mu\}_k \in S_k} E_{\{\mu\}_k}(\cdot)E_{\{\mu\}_k}^\dagger$, where the set $\mathbf{S}_k$ is the set of all error configurations $\{\mu\}_k$ with k physical errors. Note that $\mathcal{Q}_1 = \mathcal{E}_1$, where $\mathcal{E}_1(\cdot) = \frac{1}{N} \sum_\mu E_\mu(\cdot)E_\mu^\dagger$ is the total error channel defined in the Lindbladian in Eq. (104) and N is the total number of error jumps in the Lindbladian.

Let us consider the channel $\mathcal{Q}_1^k$. The product expands into a convex combination of terms that contain a different number of E_μ's. Since the channel is symmetric under permutation

of the error indices, all the terms with the same number of E_μ's will have the same coefficient. In particular, this implies that, for any integer $k \geq 0$,

$$\mathcal{Q}_1^k = \sum_{i=0}^k r_{ki} \mathcal{Q}_i, \tag{129}$$

where $r_{ki} \geq 0$ and $\sum_i r_{ki} = 1$.

We consider the class of n-qubit error-correcting codes C with a varying distance $d = d(n)$ that satisfy the following: There exists an integer-valued function $h = h(n) > 0$ such that for $k \leq h$ and any $|\psi\rangle \in \mathsf{C}$, the following holds:

$$\mathcal{R}\mathcal{Q}_k |\psi\rangle\langle\psi| - (1 - \xi)|\psi\rangle\langle\psi| \geq 0, \tag{130}$$

where $\xi = 2^{-\Omega(d)}$ and is independent of $|\psi\rangle$. It follows that

$$\mathcal{R}\mathcal{Q}_1^k |\psi\rangle\langle\psi| = \sum_{i=0}^k r_{ki} \mathcal{R}\mathcal{Q}_i |\psi\rangle\langle\psi| \geq (1 - \xi)|\psi\rangle\langle\psi|. \tag{131}$$

Note that $h(n)$ is a tolerable error weight for C. For example, if we let $h = \ell$, where ℓ is the error radius satisfying $d = 2\ell + 1$, then we have $\xi = 0$. Moreover, if there exists a constant $f > 0$ such that $nf \leq h$ for all n, then for $k \leq nf$, the code we consider has a threshold according to Definition 2. This set of codes is not very restricted and contains commonly known examples, e.g. the quantum stabilizer codes subject to single-qubit Pauli noise.

We now proceed to prove Theorem 3. We first prove the following lemma:

Lemma 4. *Assume an n-qubit code family with increasing n and a tolerable error weight $h = h(n)$ with respect to the error channel defined above. Then $p_e(k)$ in Eq. (106) satisfies*

$$p_e(k) \leq 1 - [(1 - \xi)(1 - p_1 s_1)]^k, \tag{132}$$

where $\xi = 2^{-\Omega(d)}$ and s_1 is the solution to the recurrence relation

$$s_v = \frac{v}{N} p_1 s_{v-1} + \left(1 - \frac{v}{N}\right) p_1 s_{v+1}, \quad s_0 = 0, \quad s_{h+1} = 1, \tag{133}$$

with $p_1 = \frac{N\Delta}{\kappa + N\Delta}$.

Proof. Our goal is to lower-bound the contribution $\min_{\rho_0} \sum_{\{\mathbf{a}\}} p_{a_1} p_{a_2} \cdots p_{a_k} \mathrm{Tr} \left[\rho_0 \mathcal{R} \mathcal{E}_{a_1} \mathcal{E}_{a_2} \cdots \mathcal{E}_{a_k} \rho_0\right]$ contained in $p_e(k)$ (defined below Eq. (106)), where $\{\mathbf{a}\}$ is the set of length-k trajectories $\mathbf{a} = (a_1, a_2, \cdots, a_k)$ with the labels $a_i \in \{0, 1\}$. For a given jump sequence $\mathbf{a}$, we can write

$$p_{a_1} p_{a_2} \cdots p_{a_k} \mathrm{Tr} \left[\rho_0 \mathcal{R} \mathcal{E}_{a_1} \mathcal{E}_{a_2} \cdots \mathcal{E}_{a_k} \rho_0\right] = (p_1^{m_0})(p_0 p_1^{m_1}) \cdots (p_0 p_1^{m_z}) \mathrm{Tr} \left[\rho_0 \mathcal{R} \mathcal{E}_1^{m_0} \cdots \mathcal{R} \mathcal{E}_1^{m_z} \rho_0\right], \tag{134}$$

where z denotes the number of 0's in the sequence $\mathbf{a} = (a_1, \cdots, a_k)$ and $z + \sum_{i=0}^z m_i = k$. Note that the sequence $\mathbf{a}$ is also uniquely labelled by $\mathbf{m}(\mathbf{a}) = (m_0, m_1, \cdots, m_z)$. We use

Eq. (129) to decompose the error subsequence

$$(p_1^{m_0})(p_0 p_1^{m_1}) \cdots (p_0 p_1^{m_z}) \text{Tr} \left[\rho_0 \mathcal{R} \mathcal{E}_1^{m_0} \cdots \mathcal{R} \mathcal{E}_1^{m_z} \rho_0 \right]$$

$$= \left(p_1^{m_0} \sum_{i_0=0}^{m_0} r_{m_0 i_0} \right) \left(p_0 p_1^{m_1} \sum_{i_1=0}^{m_1} r_{m_1 i_1} \right) \cdots \left(p_0 p_1^{m_z} \sum_{i_z=0}^{m_z} r_{m_z i_z} \right) \text{Tr} \left[\rho_0 \mathcal{R} \mathcal{Q}_{i_0} \mathcal{R} \mathcal{Q}_{i_1} \cdots \mathcal{R} \mathcal{Q}_{i_z} \rho_0 \right]$$

$$\geq (1-\xi)^k \left(p_1^{m_0} \sum_{i_0=0}^{\min\{h,m_0\}} r_{m_0 i_0} \right) \left(p_0 p_1^{m_1} \sum_{i_1=0}^{\min\{h,m_1\}} r_{m_1 i_1} \right) \cdots \left(p_0 p_1^{m_z} \sum_{i_z=0}^{\min\{h,m_z\}} r_{m_z i_z} \right)$$

$$= (1-\xi)^k \sum_{i_0=0}^{\min\{h,m_0\}} \sum_{i_1=0}^{\min\{h,m_1\}} \cdots \sum_{i_z=0}^{\min\{h,m_z\}} \left(p_1^{m_0} r_{m_0 i_0} \right) \left(p_0 p_1^{m_1} r_{m_1 i_1} \right) \cdots \left(p_0 p_1^{m_z} r_{m_z i_z} \right). \tag{135}$$

In the second line, we restricted the sums and used the fact that

$$\text{Tr} \left[\rho_0 \mathcal{R} \mathcal{Q}_{i_0} \mathcal{R} \mathcal{Q}_{i_1} \cdots \mathcal{R} \mathcal{Q}_{i_z} \rho_0 \right] \geq (1-\xi)^k, \tag{136}$$

which follows from Eq. (130) using the same reasoning as the one used to derive Eq. (112).

To proceed, we note that the decomposition in Eq. (129) can be interpreted as a random-walk process that either creates or annihilates an error at each step. Each jump randomly applies one of the N different errors. The same error cancels with itself if it is triggered an even number of times. Let v be the number of physical errors at the current configuration (i.e. $E_{\{\mu\}} |\psi\rangle\langle\psi| E_{\{\mu\}}^\dagger$ with a subset of error indices satisfying $|\{\mu\}| = v$ and some fixed reference logical state $|\psi\rangle$). The next jump has a probability of $1 - v/N$ to create a physical error or a probability of v/N to cancel a physical error. At each step, the number of physical errors will be updated accordingly. For example,

$$\mathcal{Q}_1 \mathcal{Q}_1 = 1 \cdot \frac{1}{N} \cdot \mathcal{Q}_0 + 1 \cdot \frac{N-1}{N} \cdot \mathcal{Q}_2, \tag{137}$$

where $\mathcal{Q}_2(\cdot) = \frac{1}{N(N-1)} \sum_\mu \sum_{\mu' \neq \mu} E_\mu E_{\mu'}(\cdot) E_{\mu'}^\dagger E_\mu^\dagger$. That is, when applying $\mathcal{Q}_1$ twice, there are two possible paths for the errors: (i) The first jump creates an error, and the second jump cancels the created error; (ii) The first jump creates an error, and the second jump creates another error. Similarly, we have $\mathcal{Q}_2 \mathcal{Q}_1 = \frac{2}{N} \mathcal{Q}_1 + \frac{N-2}{N} \mathcal{Q}_3$. This leads to three paths:

$$\mathcal{Q}_1 \mathcal{Q}_1 \mathcal{Q}_1 = 1 \cdot \frac{1}{N} \cdot 1 \cdot \mathcal{Q}_1 + 1 \cdot \frac{N-1}{N} \cdot \frac{2}{N} \cdot \mathcal{Q}_1 + 1 \cdot \frac{N-1}{N} \cdot \frac{N-2}{N} \cdot \mathcal{Q}_3. \tag{138}$$

The three terms correspond to the three possible paths when applying $\mathcal{Q}_1$ three times. This suggests that each coefficient r_{ki} in Eq. (129) takes the form

$$r_{mi} = \sum_{\{\mathbf{v}(m,i)\}} g(v_0, v_1) \cdots g(v_{m-1}, v_m), \tag{139}$$

where $\{\mathbf{v}(m,i)\}$ is the set of all paths that lead to i physical errors when $\mathcal{Q}_1$ is applied m times. Here $\mathbf{v}(m,i) = (v_0, v_1, v_2, \cdots, v_m)$, where v_j is the number of physical errors after the j-th jump. By definition, $v_0 = 0$ and $v_m = i$. The coefficient $g(v_{j-1}, v_j)$ is the probability

that v_j errors are present after the j-th jump, conditioned on the presence of v_{j-1} errors after the $(j-1)$-th jump. Explicitly, we have, for $j \geq 1$,

$$g(v_{j-1}, v_j) = \begin{cases} \frac{v_{j-1}}{N} & \text{if } v_j - v_{j-1} = -1, \\ 1 - \frac{v_{j-1}}{N} & \text{if } v_j - v_{j-1} = 1. \end{cases} \tag{140}$$

The goal is to lower-bound the contribution $\min_{\rho_0} \sum_{\{\mathbf{a}\}} p_{a_1} p_{a_2} \cdots p_{a_k} \mathrm{Tr}\left[\rho_0 \mathcal{R} \mathcal{E}_{a_1} \mathcal{E}_{a_2} \cdots \mathcal{E}_{a_k} \rho_0\right]$ from Eq (106). Summing over all possible length-k trajectories $\{\mathbf{a}\}$ is the same as summing over $\{\mathbf{m}(\mathbf{a})\}$, which labels each trajectory in $\{\mathbf{a}\}$ uniquely by the integer sequence $(m_0, \cdots, m_z)$. Summing Eq. (135) over $\{\mathbf{m}(\mathbf{a})\}$ and using Eq. (139) leads to

$$\sum_{\{\mathbf{m}(\mathbf{a})\}} \sum_{i_0=0}^{\min\{h,m_0\}} \sum_{i_1=0}^{\min\{h,m_1\}} \cdots \sum_{i_z=0}^{\min\{h,m_z\}} \left(p_1^{m_0} r_{m_0 i_0}\right) \left(p_0 p_1^{m_1} r_{m_1 i_1}\right) \cdots \left(p_0 p_1^{m_z} r_{m_z i_z}\right)$$

$$= \sum_{\{\mathbf{m}(\mathbf{a})\}} \sum_{i_0=0}^{\min\{h,m_0\}} \sum_{i_1=0}^{\min\{h,m_1\}} \cdots \sum_{i_z=0}^{\min\{h,m_z\}} \sum_{\{\mathbf{v}(m_0,i_0)\}} \sum_{\{\mathbf{v}(m_1,i_1)\}} \cdots \sum_{\{\mathbf{v}(m_z,i_z)\}}$$
$$\left(\prod_{j=1}^{m_0} p_1 g(v_{j-1}, v_j)\right) p_0 \left(\prod_{j=1}^{m_1} p_1 g(v_{j-1}, v_j)\right) p_0 \cdots \left(\prod_{j=1}^{m_z} p_1 g(v_{j-1}, v_j)\right)$$

$$\geq \sum_{\{\mathbf{m}(\mathbf{a})\}} \sum_{i_0=0}^{\min\{h,m_0\}} \sum_{i_1=0}^{\min\{h,m_1\}} \cdots \sum_{i_z=0}^{\min\{h,m_z\}} \sum_{\{\mathbf{v}_h(m_0,i_0)\}} \sum_{\{\mathbf{v}_h(m_1,i_1)\}} \cdots \sum_{\{\mathbf{v}_h(m_z,i_z)\}}$$
$$\left(\prod_{j=1}^{m_0} p_1 g(v_{j-1}, v_j)\right) p_0 \left(\prod_{j=1}^{m_1} p_1 g(v_{j-1}, v_j)\right) p_0 \cdots \left(\prod_{j=1}^{m_z} p_1 g(v_{j-1}, v_j)\right), \tag{141}$$

where in the last inequality we restrict the sum to the subset $\{\mathbf{v}_h(m,i)\} \subseteq \{\mathbf{v}(m,i)\}$ of paths along which the number of physical errors v always satisfies $v \leq h$. Each term in the sum is a product of k jump probabilities for a random-walk trajectory specified by the sequence $(\mathbf{v}_h(m_0, i_0), \cdots, \mathbf{v}_h(m_z, i_z))$. To proceed, let us now define a random walk according to the rules in Eq. (139): Given a configuration with v physical errors, the random walk updates with one of the three stochastic jumps:

1. With probability $p_1(1 - \frac{v}{N})$, $v \to v+1$.
2. With probability $p_1 \frac{v}{N}$, $v \to v-1$.
3. With probability p_0, the process terminates and returns success.

After the first jump of the walk, two more termination checks (note that these are not counted as jumps) are done before each future stochastic jump is taken:

4. If $v = 0$, the process terminates and returns success.
5. If $v = h+1$, the process terminates and returns failure.

This random walk is always initialized in a configuration with zero physical errors, and the walk terminates with probability one (non-terminating trajectories have an infinite number of steps and therefore a probability of zero). To establish a lower bound for Eq. (141), we consider a stochastic process $\Phi(k)$ of k consecutive independent random-walk processes defined above. The stochastic process $\Phi(k)$ returns success if all k random walks return success. By definition, $\Phi(k)$ contains at least k jumps before it is terminated. Furthermore,

we note that the set of all possible first k jumps of a successful $\Phi(k)$ is the same as the set of trajectories in Eq. (141).

Namely, any trajectory specified by $(\mathbf{v}_h(m_0, i_0), \cdots, \mathbf{v}_h(m_z, i_z))$ in Eq. (141) is a valid trajectory for the first k jumps in a successful $\Phi(k)$, and any possible set of first k jumps taken by the process can be specified by some $(\mathbf{v}_h(m_0, i_0), \cdots, \mathbf{v}_h(m_z, i_z))$. To see this, suppose we have a trajectory for the first k jumps for a successful $\Phi(k)$. Since no more than h physical errors can be generated by the trajectory, we can find all the subsequences of jumps separated by a recovery (termination with a success) and define the corresponding $\mathbf{v}_h(m, i)$ for each subsequence. Conversely, if we have some $(\mathbf{v}_h(m_0, i_0), \cdots, \mathbf{v}_h(m_z, i_z))$, we can identify all the subsequences of jumps separated by the termination steps 3 and 4 of $\Phi(k)$, with each subsequence belonging to one of the independent random walks in $\Phi(k)$. We therefore have a one-to-one map between the two sets of trajectories. It follows that they are the same set.

This identification leads to the lower bound

$$
\sum_{\{\mathbf{m(a)}\}} \sum_{i_0=0}^{\min\{h,m_0\}} \sum_{i_1=0}^{\min\{h,m_1\}} \cdots \sum_{i_z=0}^{\min\{h,m_z\}} \sum_{\{\mathbf{v}_h(m_0,i_0)\}} \sum_{\{\mathbf{v}_h(m_1,i_1)\}} \cdots \sum_{\{\mathbf{v}_h(m_z,i_z)\}}
$$
$$
\left(\prod_{j=1}^{m_0} p_1 g(v_{j-1}, v_j) \right) p_0 \left(\prod_{j=1}^{m_1} p_1 g(v_{j-1}, v_j) \right) p_0 \cdots \left(\prod_{j=1}^{m_z} p_1 g(v_{j-1}, v_j) \right)
$$
$$
\geq \sum_{\{\mathbf{m(a)}\}} \sum_{i_0=0}^{\min\{h,m_0\}} \sum_{i_1=0}^{\min\{h,m_1\}} \cdots \sum_{i_z=0}^{\min\{h,m_z\}} \sum_{\{\mathbf{v}_h(m_0,i_0)\}} \sum_{\{\mathbf{v}_h(m_1,i_1)\}} \cdots \sum_{\{\mathbf{v}_h(m_z,i_z)\}}
$$
$$
\Pr\left(\Phi(k) \text{ returns success}|\text{First } k \text{ jumps}\right)
$$
$$
\times \left(\prod_{j=1}^{m_0} p_1 g(v_{j-1}, v_j) \right) p_0 \left(\prod_{j=1}^{m_1} p_1 g(v_{j-1}, v_j) \right) p_0 \cdots \left(\prod_{j=1}^{m_z} p_1 g(v_{j-1}, v_j) \right)
$$
$$
= \Pr\left(\Phi(k) \text{ returns success}\right), \tag{142}
$$

where the conditional probabilities are the success probability of $\Phi(k)$ conditioned on its first k stochastic jumps.

To solve for $\Pr\left(\Phi(k) \text{ returns success}\right)$, we only need to solve for the success probability of each random walk. Let us now consider a generalized random walk that follows the same rules but can start from initial configurations with any number of physical errors. Let s_v be the conditional probability that, when initialized in a configuration with $v \in [1, h]$ physical errors, the random walk terminates with failure. For mathematical convenience, we also define $s_0 = 0$ and $s_{h+1} = 1$. The probability s_v for $v \in [1, h]$ can be solved from a recurrence relation

$$
s_v = \frac{v}{N} p_1 s_{v-1} + \left(1 - \frac{v}{N}\right) p_1 s_{v+1}, \ s_0 = 0, \ s_{h+1} = 1. \tag{143}
$$

Recall that s_1 is the failure probability conditioned on an initial configuration with one physical error. To get the failure probability, we need to multiply s_1 by p_1—the probability of creating one error from a zero-error configuration. Therefore, the failure probability for a single random walk starting from a zero-error configuration is $p_1 s_1$. The success probability
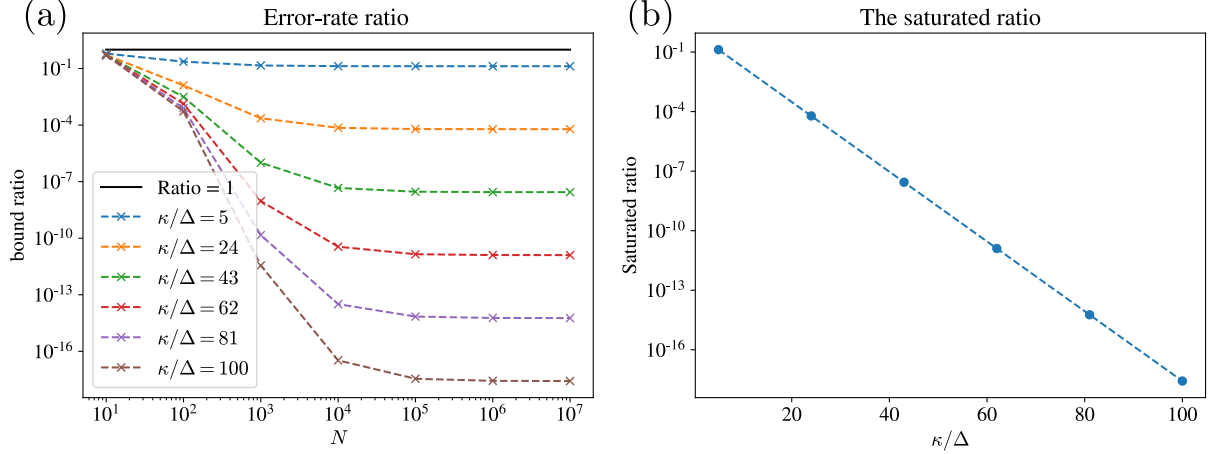
Figure 7: Numerical solutions to the error-rate ratio $s_1 / \left(\frac{N\Delta}{\kappa + N\Delta} \right)^h$ for $h = 0.4N$. (a) The log-log plot shows the ratio as a function of N for different κ/Δ. We see that the ratio for different κ/Δ eventually saturates to a constant at large N. (b) The semi-log plot shows the saturated ratio as a function of κ/Δ with a fitted line $-0.4957\kappa/\Delta + 0.0005$. Since $\lim_{N \to \infty} \left(\frac{N\Delta}{\kappa + N\Delta} \right)^{fN} = e^{-f\kappa/\Delta}$ for any constant f, the linearity of the plot of the saturated ratio suggests that s_1 has the form $\log s_1 \propto -\kappa/\Delta$ at $N \to \infty$.

for the random walk and $\Phi(k)$ are therefore $(1 - p_1 s_1)$ and $(1 - p_1 s_1)^k$, respectively. This provides a lower bound for the contribution

$$\min_{\rho_0} \sum_{\{\mathbf{a}\}} p_{a_1} p_{a_2} \cdots p_{a_k} \mathrm{Tr}\left[\rho_0 \mathcal{R} \mathcal{E}_{a_1} \mathcal{E}_{a_2} \cdots \mathcal{E}_{a_k} \rho_0 \right] \geq \left[(1 - \xi)(1 - p_1 s_1) \right]^k. \qquad (144)$$

This yields the desired bound stated in the lemma. $\qquad \square$

Plugging the bound on $p_e(k)$ from Eq. (132) into Eq. (106), we arrive at the desired bound in Theorem 3.

To understand the behaviour of the improved bound (Theorem 3) compared to the one given by Theorem 2, let us solve for s_1 numerically. We consider the ratio of error rates appearing in the two theorems: $s_1 / \left(\frac{N\Delta}{\kappa + N\Delta} \right)^h$, where $h = fN$ with $f \in (0, 1/2]$. We split the scenarios into two cases:

(i) $f < 1/2$. We evaluate the ratio for $f = 0.4$ and 0.45 for different N and different noise rates κ/Δ. In Fig. 7, we show the numerical results for $f = 0.4$. For $f = 0.45$, the plots look qualitatively the same.

(ii) $f = 1/2$. The numerical results are shown in Fig. 8.

From these numerical results, we arrive at the empirical observations presented in the main text.
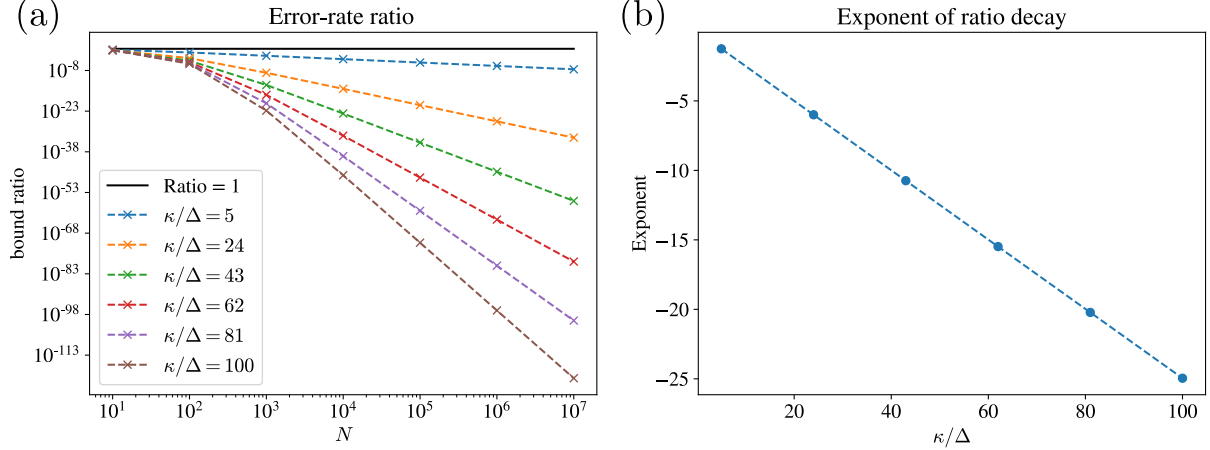
Figure 8: Numerical solutions to the error-rate ratio $s_1/\left(\frac{N\Delta}{\kappa+N\Delta}\right)^h$ for $h = N/2$. (a) The log-log plot shows the error-rate ratio as a function of N. We see in this case the ratio is steadily converging to 0 at $N \to \infty$. The linearity of the convergence suggests algebraic decay as a function of N with different exponents. (b) The plot, on a linear scale, shows the fitted exponents obtained by a linear fit to the straight lines in the error-ratio plot (a). A linear fit to the exponents yields $-0.24956\kappa/\Delta - 0.00707 \approx -\kappa/(4\Delta)$. We therefore deduce empirically that the ratio behaves as $\sim 1/N^{\kappa/(4\Delta)}$ as $N \to \infty$.

Appendix F: Proof of Theorem 4

This appendix contains the proof of Theorem 4. The proof of this theorem partially uses the proof of Theorem 1. We start with Eq. (87) which takes the form

$$\langle \Box \mathbf{e e e} \rangle = \frac{1}{s} + \frac{1}{s}\langle \Box \mathbf{e e e} \underbrace{\otimes\!\!=\!\!\otimes \ldots \otimes\!\!=\!\!\otimes}_{\ell+1} \rangle. \tag{145}$$

Next, we recall that the Poissonian error generator takes the form $\Delta\mathcal{L}_E(\rho) = N\Delta(\mathcal{E}(\rho) - \rho)$, where $\mathcal{E}(\rho) = N^{-1}\sum_{\mu=1}^N E_\mu \rho E_\mu^\dagger$ is the error superoperator. Let us use the notation

$$N\Delta\mathcal{E} = \bullet, \qquad N\Delta\mathcal{I} = \circ. \tag{146}$$

where $\mathcal{I}$ is the identity superoperator. Then, we can state the following diagrammatic relation (see Eq. (68)):

$$\otimes = \bullet - \circ. \tag{147}$$

Using the decomposition in Eqs. (76) and (147), we have

$$\langle \Box \mathbf{e e e} \rangle = \frac{1}{s} + \frac{1}{s}\langle \Box \mathbf{e e e} \underbrace{\otimes\!\!=\!\!\otimes \ldots \otimes\!\!=\!\!\otimes}_{\ell}\!\!-\!\!\bullet \rangle - \frac{1}{s}\langle \Box \mathbf{e e e} \underbrace{\otimes\!\!=\!\!\otimes \ldots \otimes\!\!=\!\!\otimes}_{\ell}\!\!-\!\!\circ \rangle + \frac{1}{s}\langle \Box \mathbf{e e e} \underbrace{\otimes\!\!=\!\!\otimes \ldots \otimes\!\!=\!\!\otimes}_{\ell}\!\!\to\!\!\otimes \rangle. \tag{148}$$

Taking into account that $\mathcal{W}_t = e^{-\kappa t}\mathcal{I}$ for global decoder, the first terms can be rewritten as

$$\frac{1}{s}\langle \Box \mathbf{e e e} \underbrace{\otimes\!\!=\!\!\otimes \ldots \otimes\!\!=\!\!\otimes}_{\ell}\!\!-\!\!\bullet \rangle = \frac{1}{s(s+\kappa)}\langle \Box \mathbf{e e e} \underbrace{\otimes\!\!=\!\!\otimes \ldots \otimes\!\!=\!\!\otimes}_{\ell}\!\!\bullet \rangle. \tag{149}$$

40

Using Eq. (85), we can rewrite the second term as

$$\frac{1}{s}\Big\langle \Box\!\!\mathit{eee}\underbrace{\otimes\!\!=\!\!\otimes\ldots\otimes\!\!=\!\!\otimes}_{\ell}\!\!-\!\!\circ\Big\rangle = \frac{N\Delta}{s(s+\kappa)}\Big\langle \Box\!\!\mathit{eee}\underbrace{\otimes\!\!=\!\!\otimes\ldots\otimes\!\!=\!\!\otimes}_{\ell}\Big\rangle = \frac{N\Delta}{s(s+\kappa)}\Big\langle \Box\!\!\mathit{eee}\underbrace{\otimes\!\!=\!\!\otimes\ldots\otimes\!\!=\!\!\otimes}_{\ell+1}\Big\rangle. \tag{150}$$

The last term in Eq. (148) vanishes due to Lemma 2.

By combining these results, we reach the conclusion that

$$\Big\langle \Box\mathit{eee}\Big\rangle = \frac{1}{s} + \frac{1}{s(s+\kappa)}\Big\langle \Box\mathit{eee}\underbrace{\otimes\!\!=\!\!\otimes\ldots\otimes\!\!=\!\!\otimes}_{\ell}\bullet\Big\rangle - \frac{N\Delta}{s(s+\kappa)}\Big\langle \Box\mathit{eee}\underbrace{\otimes\!\!=\!\!\otimes\ldots\otimes\!\!=\!\!\otimes}_{\ell+1}\Big\rangle. \tag{151}$$

Subsequently, by utilizing Eq. (87), we can express

$$\frac{1}{s}\Big\langle \Box\mathit{eee}\underbrace{\otimes\!\!=\!\!\otimes\ldots\otimes\!\!=\!\!\otimes}_{\ell+1}\Big\rangle = \Big\langle \Box\mathit{eee}\Big\rangle - \frac{1}{s}. \tag{152}$$

After rearranging the terms, we obtain

$$\Big\langle \Box\mathit{eee}\Big\rangle\left(1 + \frac{N\Delta}{s+\kappa}\right) = \frac{1}{s}\left(1 + \frac{N\Delta}{s+\kappa}\right) + \frac{1}{s(s+\kappa)}\Big\langle \Box\!\!=\!\!\underbrace{\otimes\!\!=\!\!\otimes\ldots\otimes\!\!=\!\!\otimes}_{\ell}\bullet\Big\rangle. \tag{153}$$

Lastly, by dividing both sides of the equation by $(1 + N\Delta/(s+\kappa))$, we arrive at

$$\Big\langle \Box\mathit{eee}\Big\rangle = \frac{1}{s} + \frac{1}{s(s+\kappa+N\Delta)}\Big\langle \Box\mathit{eee}\underbrace{\otimes\!\!=\!\!\otimes\ldots\otimes\!\!=\!\!\otimes}_{\ell}\bullet\Big\rangle. \tag{154}$$

By repeating this procedure ℓ times, we obtain the expression

$$\Big\langle \Box\mathit{eee}\Big\rangle = \frac{1}{s} + \frac{1}{s(s+\kappa+N\Delta)^\ell}\Big\langle \Box\mathit{eee}\bullet^{\ell+1}\Big\rangle. \tag{155}$$

The explicit form of the inverse Laplace transform of this equation can be obtained as

$$\mathscr{L}^{-1}\Big\langle \Box\mathit{eee}\bullet^{\ell+1}\Big\rangle = \frac{1}{2}(N\Delta)^{\ell+1}\mathrm{Tr}\Big[Q\exp(\mathcal{L}t)\mathcal{E}^{\ell+1}(\delta\rho)\Big]. \tag{156}$$

As $\mathcal{E}$ and $\exp(\mathcal{L}t)$ are completely positive trace-preserving (CPTP) maps that do not alter the matrix norm, we can put a lower bound on

$$\mathrm{Tr}\Big[Q\exp(\mathcal{L}t)\mathcal{E}^{\ell+1}(\delta\rho)\Big] = \mathrm{Tr}\Big[Q\exp(\mathcal{L}t)\mathcal{E}^{\ell+1}(|0\rangle\langle 0|)\Big] - \mathrm{Tr}\Big[Q\exp(\mathcal{L}t)\mathcal{E}^{\ell+1}(|1\rangle\langle 1|)\Big]$$
$$\geq -2\|Q\| = -2. \tag{157}$$

Thus we get

$$\mathscr{L}^{-1}\Big\langle \Box\mathit{eee}\bullet^{\ell+1}\Big\rangle \geq -(N\Delta)^{\ell+1}. \tag{158}$$

Then we derive the bound

$$\mathscr{L}^{-1}\Big\langle \Box\mathit{eee}\Big\rangle \geq 1 - (N\Delta)^{\ell+1}\mathscr{L}^{-1}\left\{\frac{1}{s^2(s+\kappa+N\Delta)^\ell}\right\}. \tag{159}$$

Taking the inverse Laplace transform, we get

$$\epsilon(t), \delta(t) \leq \frac{1}{(1+\kappa/N\Delta)^{\ell+1}}F\Big((\kappa+N\Delta)t\Big). \tag{160}$$

This expression concludes our proof.

Appendix H: Dissipative toric code

In this appendix, we closely examine the Lindblad operator for the autonomous decoder based on the two-dimensional toric code as described in Section 5. We demonstrate that, in the absence of noise, the recovery Lindblad operator in Eq. (8) is exactly solvable. We use these solutions to perturbatively derive the spectral gap of the full operator.

For simplicity, we will limit our analysis to the case in which only star excitations are allowed, i.e., no plaquettes are excited. Despite this, we emphasize that our main conclusions should hold in the presence of both types of excitations. We will consider noise models where the eigenvalues of B_p are always good quantum numbers, and focus our attention on the gauge sector where $B_p = +1$ for all p, i.e., the subspace that contains the ground states. The reduced Hilbert space will consist of states that have an even number of star excitations. We choose the following labeling convention for states that span the reduced Hilbert space:

$$|0,0;\mathbf{0}\rangle = \prod_i (1 + A_i)|\mathrm{vac}\rangle, \qquad |r,s;\mathbf{0}\rangle = (g_x)^r (g_y)^s |0,0;\mathbf{0}\rangle, \qquad |r,s,\mathbf{k}\rangle = \left(\prod Z\right)_{\mathbf{k}} |r,s,\mathbf{0}\rangle, \tag{161}$$

where A_i represents different star operators, $|\mathrm{vac}\rangle$ is the ground state of all Z_j operators: $Z_j|\mathrm{vac}\rangle = |\mathrm{vac}\rangle$; $r,s \in 0,1$ label different topological sectors; $g_{x/y} = \Pi_{\mathrm{hor/vert}} X$ is a product of X operators along a string (on the dual lattice) that wraps around the horizontal/vertical direction of the torus. It is easy to check that $|r,s;\mathbf{0}\rangle$ are orthogonal ground states of H (they are $+1$ eigenstates of all the A_s and B_p). Excited states $|r,s,\mathbf{k}\rangle$ are labeled by $\mathbf{k}$. For a system with $L \times L$ stars, $\mathbf{k}$ is an L^2-dimensional vector that labels the excited stars with 1 and de-excited stars with 0. Excited eigenstates are defined by applying strings of $(\prod Z)$ operators on the ground state via the smallest number of Z operators. When there are multiple minimal-weight excitation operators, then a $(\prod Z)_{\mathbf{k}}$ operator is chosen arbitrarily from the various options.

We consider the following recovery map:

$$\mathcal{R}(\rho) = \sum_{\mathbf{k}} K_{\mathbf{k}} \rho K_{\mathbf{k}}^\dagger, \qquad K_{\mathbf{k}} = \left(\prod Z\right)_{\mathbf{k}} P_{\mathbf{k}}, \tag{162}$$

where $P_{\mathbf{k}} = \Pi_j (1 + (-1)^{k_j} A_j)$ is a projector onto a given star configuration $\mathbf{k}$, and $(\prod Z)_{\mathbf{k}}$ is an operator that "fixes" the error using the minimal number of Z operators. In other words, $K_{\mathbf{k}}|r,s;\mathbf{k}\rangle = |r,s;\mathbf{0}\rangle$. Note that the number of star configurations is 2^{L^2-1}, which means that the number of dissipators scales exponentially with system size. Note also that the dissipators are non-local, i.e. they have support on the full lattice. Nevertheless, there is still a notion of locality: The dissipators fix star errors via strings of Z operators which minimize the total path length between excited stars, a process known as minimal weight matching.

One can easily check that arbitrary superpositions of toric code ground states are the *only* steady states of the system. It is thus clear that this idealized limit hosts a qudit steady-state structure. We now ask how stable this degeneracy is with respect to dephasing perturbations, which act on each physical qubit, i.e. how quickly do "coherences" decay in the presence of dephasing. To this end, we introduce the following dissipators on each edge of the lattice:

$$E_\mu = Z_\mu. \tag{163}$$

Let us reformulate the question more precisely. We begin by noting that the jump operators $\{K_{\mathbf{k}}, E_\mu\}$ commute with B_p, and hence indeed it makes sense to focus on the gauge sector with $B_p = +1$ for all p. Even within this gauge sector, we can further partition the subspace into different "topological sectors". Let us define the following projection operators:

$$P_{rs} = \sum_{\mathbf{k}} |r, s; \mathbf{k}\rangle\langle r, s; \mathbf{k}|, \tag{164}$$

where $r, s \in 0, 1$ and P_{rs} projects states into topological sector r, s. We now note that all of the dissipators commute with P_{rs}. Thus these projectors are "strong symmetries" of the Lindbladian [70], and hence there exists a basis where the Lindbladian in Eq. (9) is be block-diagonalized and consists $4^2 = 16$ different blocks:

$$\mathcal{L} = \text{Diag}[\mathcal{L}_{0,0}, \mathcal{L}_{0,1}, \mathcal{L}_{0,2}, \ldots \mathcal{L}_{3,3}], \tag{165}$$

where the numbers 0 to 3 label four different topological sectors of the bras and kets accoding to the convention $(r = 0, s = 0) \to 0$, $(r = 1, s = 0) \to 1$, $(r = 0, s = 1) \to 2$, $(r = 1, s = 1) \to 3$. In words, the Lindbladian $\mathcal{L}_{0,0}$ acts on operators where both ket and bra belong to the same topological sector $r = 0, s = 0$; on the other hand, $\mathcal{L}_{0,1}$ acts on operators where the ket belongs to sector $r = 0, s = 0$, while the bra belongs to sector $r = 1, s = 0$. Operators belonging to different topological sectors evolve independently.

We now show that, in the absence of dephasing ($\Delta = 0$), the model is exactly solvable, meaning that we can write down exact expressions for the right and left eigenoperators of the Lindbladian in each topological sector and its spectrum. Let us define right and left eigenoperators of the Lindbladian:

$$\mathcal{L}_{p,q}(r_{p,q;m}) = \Lambda_m r_{p,q;m}, \qquad \mathcal{L}_{p,q}^\dagger(l_{p,q;m}) = \Lambda_m^* l_{p,q;m}, \tag{166}$$

where p, q label the topological sector, and m represents different eigenvalues within a given sector (it turns out that the spectrum is the same in all sectors in this limit, so we suppress the topological labels on Λ).

For $\Delta = 0$, each topological sector has exactly one eigenvalue of zero: $\Lambda_0 = 0$. One can show that the corresponding eigenoperators are

$$r_{p,q;0} = |p; \mathbf{0}\rangle\langle q; \mathbf{0}|, \qquad l_{p,q;0} = \sum_{\mathbf{k}} |p; \mathbf{k}\rangle\langle q; \mathbf{k}|. \tag{167}$$

This ensures that arbitrary *superpositions* of toric code ground states are indeed steady states of the model:

$$|\psi\rangle = \sum_{p=0}^{3} c_p |p; \mathbf{0}\rangle, \qquad \mathcal{L}(|\psi\rangle\langle\psi|) = 0, \quad \forall \sum_{p=0}^{3} |c_p|^2 = 1. \tag{168}$$

The full Lindbladian $\mathcal{L}$ therefore has $4^2 = 16$ eigenvalues of zero. In a slight abuse of notation, we shall call this a "qubit steady state structure". (Rather than a qudit steady state structure.)

We now turn to "diagonal" eigenoperators which come with a decay rate: $\Lambda_{\mathbf{k}} = -\kappa$. The corresponding eigenoperators are

$$r_{p,q;\mathbf{k}} = |p;\mathbf{k}\rangle\langle q;\mathbf{k}| - |p;\mathbf{0}\rangle\langle q;\mathbf{0}|, \qquad l_{p,q;\mathbf{k}} = |p;\mathbf{k}\rangle\langle q;\mathbf{k}|. \tag{169}$$

It is clear that $\text{tr}\,[r_{p,q;\mathbf{k}}] = 0$ and $\text{tr}\,[l^{\dagger}_{p,q;\mathbf{k}} r_{p,q;\mathbf{k}}] = 1$, which are necessary conditions.

Finally, we turn to off-diagonal eigenoperators which come with a decay rate: $\Lambda_{\mathbf{k},\mathbf{k}'} = -\kappa$. The corresponding eigenoperators are:

$$r_{p,q;\mathbf{k},\mathbf{k}'} = |p;\mathbf{k}\rangle\langle q;\mathbf{k}'|, \qquad l_{p,q;\mathbf{k},\mathbf{k}'} = |p;\mathbf{k}\rangle\langle q;\mathbf{k}'|. \tag{170}$$

In this case, the right and left eigenoperators happen to be identical.

Perturbative results

Having found the exact expressions for all of the right and left eigenoperators of the Lindbladian in the absence of dephasing $\Delta = 0$, we would now like to use perturbation theory to examine the effects of small dephasing $\Delta > 0$. In particular, we would like to know the fate of the qubit steady state structure, i.e. whether the Lindbladian with weak dephasing has 16 eigenvalues of zero in the thermodynamic limit.

The Lindbladian can be block diagonalized into different topological sectors (see Eq. (165)) even in the presence of dephasing. Note that all operators with non-zero trace must belong to one of the diagonal sectors $\mathcal{L}_{q,q}$, while the off-diagonal sectors act on operators with zero trace. Since it is possible to initialize a valid (traceful) density matrix in each of the diagonal sectors $\mathcal{L}_{q,q}$, we know that (even in the presence of dephasing) each of these sectors must have an eigenvalue of zero corresponding to the steady state in each topological sector. The full Lindbladian $\mathcal{L}$ is thus guaranteed to have at least four eigenvalues of zero even in the presence of Z-dephasing. The off-diagonal sectors $\mathcal{L}_{p,q}$ are not guaranteed steady state solutions in general. However, from the exact diagonalization above, we know that, in the absence of dephasing, these sectors will have an eigenvalue of zero, since arbitrary *superpositions* of toric code ground states are stable (e.g. $\mathcal{L}(|0;\mathbf{0}\rangle\langle 1;\mathbf{0}|) = 0$). We wish to understand how the decay rate of these off-diagonal coherences scales with system size in the presence of dephasing; in particular, we would like to know if the decay rate scales to zero in the thermodynamic limit.

Let us specialize to an off-diagonal sector $\mathcal{L}_{p,q}$ (we shall suppress the topological indices henceforth) and examine the shift to the eigenvalue $\Lambda_0 = 0$ via perturbation theory. The corrections (up to third order) read

$$\delta\Lambda^{(1)} = \langle l_0|\mathcal{L}'|r_0\rangle, \tag{171}$$

$$\delta\Lambda^{(2)} = \sum_{m\neq 0} \frac{\langle l_0|\mathcal{L}'|r_m\rangle\langle l_m|\mathcal{L}'|r_0\rangle}{\Lambda_0 - \Lambda_m} = \frac{1}{\kappa}\left(\langle l_0|\mathcal{L}'^2|r_0\rangle - \langle l_0|\mathcal{L}'|r_0\rangle^2\right), \tag{172}$$

$$\delta\Lambda^{(3)} = \sum_{m_1\neq 0}\sum_{m_2\neq 0} \frac{\langle l_0|\mathcal{L}'|r_{m_1}\rangle\langle l_{m_1}|\mathcal{L}'|r_{m_2}\rangle\langle l_{m_2}|\mathcal{L}'|r_0\rangle}{(\Lambda_0 - \Lambda_{m_1})(\Lambda_0 - \Lambda_{m_2})} - \delta\Lambda_1\sum_{m\neq 0} \frac{\langle l_0|\mathcal{L}'|r_m\rangle\langle l_m|\mathcal{L}'|r_0\rangle}{(\Lambda_0 - \Lambda_m)^2} \tag{173}$$

$$= \frac{1}{\kappa^2}\left(\langle l_0|\mathcal{L}'^3|r_0\rangle - 3\langle l_0|\mathcal{L}'|r_0\rangle\langle l_0|\mathcal{L}'^2|r_0\rangle + 2\langle l_0|\mathcal{L}'|r_0\rangle^3\right), \tag{174}$$

where we use the shorthand $\langle l|\mathcal{L}'|r\rangle \equiv \mathrm{tr}\,[l^\dagger \mathcal{L}'(r)]$, and

$$\mathcal{L}'(\rho) = \sum_i \left(Z_i \rho Z_i - \rho \right) \tag{175}$$

is the dephasing perturbation. We have simplified some of the general expressions by noting that the relevant excited eigenvalues are all $\Lambda_m = -\kappa$ and $\Lambda_0 = 0$. Examining the expressions for the eigenvalue shift, it is clear that, if $\langle l_0|(\mathcal{L}')^x|r_0\rangle = 0$ for all $x \leq y$, then $\delta\Lambda^{(y)} = 0$.

One-dimensional system.—Let's consider a $1 \times L$ lattice where $L = 2j+1, j \in \mathbb{Z}$, such that L is odd. We define two different toric code ground states via $|2; \mathbf{0}\rangle = X_1|0; \mathbf{0}\rangle$, where X_1 is a global loop on the dual lattice in the vertical direction (in this case, the vertical direction has length 1 so the global loop is a single operator). We define the right and left eigenoperators in the unperturbed limit:

$$r_0 = |2; \mathbf{0}\rangle\langle 0; \mathbf{0}|, \qquad l_0 = \sum_{\mathbf{k}} |2; \mathbf{k}\rangle\langle 0; \mathbf{k}|. \tag{176}$$

We next define the perturbation

$$\mathcal{L}'(\rho) = \mathcal{Z}(\rho) - L\rho, \qquad \mathcal{Z}(\rho) = \sum_{i=1}^{L} Z_i \rho Z_i, \tag{177}$$

where Z_i act only on the horizontal edges of the lattice.

Consider the first term in the perturbation theory:

$$\mathrm{tr}\,[l_0^\dagger \mathcal{L}'(r_0)] = \sum_{\mathbf{k}} \mathrm{tr}[|0, \mathbf{k}\rangle\langle 2; \mathbf{k}| \left(\mathcal{Z}(|2, \mathbf{0}\rangle\langle 0, \mathbf{0}|) - L|2, \mathbf{0}\rangle\langle 0, \mathbf{0}| \right)] \tag{178}$$

$$= -L + \sum_{\mathbf{k}} \langle 2; \mathbf{k}|\mathcal{Z}(|2, \mathbf{0}\rangle\langle 0, \mathbf{0}|)|0, \mathbf{k}\rangle] \tag{179}$$

$$= -L + L = 0. \tag{180}$$

To order α, we find

$$\mathrm{tr}\,[l_0^\dagger (\mathcal{L}')^\alpha (r_0)] = \sum_{i=0}^{\alpha} \binom{\alpha}{i} (-L)^{\alpha-i} \sum_{\mathbf{k}} \langle 2; \mathbf{k}|\mathcal{Z}^i(|2, \mathbf{0}\rangle\langle 0, \mathbf{0}|)|0, \mathbf{k}\rangle, \tag{181}$$

where we have introduced the binomial coefficient. We now note that, for $i \leq j$,

$$\sum_{\mathbf{k}} \langle 2; \mathbf{k}|\mathcal{Z}^i(|2, \mathbf{0}\rangle\langle 0, \mathbf{0}|)|0, \mathbf{k}\rangle = L^i, \qquad \text{for: } i \leq j. \tag{182}$$

This implies

$$\mathrm{tr}\,[l_0^\dagger (\mathcal{L}')^\alpha (r_0)] = L^2 \sum_{i=0}^{\alpha} \binom{\alpha}{i} (-1)^{\alpha-i} 1^i = 0, \qquad \text{for: } \alpha \leq j, \tag{183}$$

where we have used a property of binomial coefficients.

We need to be careful at order $\alpha = j + 1$. In this case,

$$\sum_{\mathbf{k}} \langle 2; \mathbf{k} | \mathcal{Z}^{j+1}(|2, \mathbf{0}\rangle\langle 0, \mathbf{0}|)|0, \mathbf{k}\rangle = L^{j+1} - 2\left(\frac{L!}{j!}\right). \tag{184}$$

The term with the factorial is counting the number of configurations with $j + 1$ excited edges which have a logical error after applying the recovery jump operators $L_{\mathbf{k}}$. This implies

$$\mathrm{tr}\,[l_0^\dagger(\mathcal{L}')^{j+1}(r_0)] = -2\left(\frac{L!}{j!}\right). \tag{185}$$

This is the lowest-order non-trivial recovery.

This implies that the contribution to the eigenvalue at this order is

$$\Lambda/\kappa = -2\left(\frac{L!}{(L/2)!}\right)\left(\frac{\Delta}{\kappa}\right)^{L/2} + O((\Delta/\kappa)^{L/2+1}), \tag{186}$$

where we have used $j + 1 \approx L/2$. We note that this term blows up in the thermodynamic limit $L \to \infty$, since the factorial term grows faster than the exponential term decays. One way to remedy this is to increase the dissipation linearly with the system size: $\kappa = \kappa_0 L$. Then the thermodynamic limit is well-defined:

$$\lim_{L\to\infty} \left(\frac{L!}{(L/2)!}\right)\left(\frac{\Delta}{\kappa_0 L}\right)^{L/2} = 0 \tag{187}$$

for $\Delta/\kappa_0 \ll 1$ such that the recovery to the eigenvalue goes to zero in the thermodynamic limit.

Two-dimensional system.—A similar analysis can be done for a 2D system on an $L \times L$ lattice. We consider a perturbation

$$\mathcal{L}'(\rho) = \mathcal{Z}(\rho) - 2L^2\rho, \qquad \mathcal{Z}(\rho) = \sum_{i=1}^{2L^2} Z_i\rho Z_i, \tag{188}$$

where Z_i act on each of the $2L^2$ edges of the lattice.

Again, the lowest-order contribution comes at order $j + 1$:

$$\mathrm{tr}\,[l_0^\dagger(\mathcal{L}')^{j+1}(r_0)] = -2L\left(\frac{L!}{j!}\right), \tag{189}$$

where this factor basically counts the number of configurations with $j + 1$ excited edges, which have a logical error after applying the recovery jump operators $L_{\mathbf{k}}$.

The recovery to the eigenvalue at this order is

$$\Lambda/\kappa = -2L\left(\frac{L!}{(L/2)!}\right)\left(\frac{\Delta}{\kappa}\right)^{L/2} + O((\Delta/\kappa)^{L/2+1}). \tag{190}$$

Again, this term blows up in the thermodynamic limit $L \to \infty$, since the factorial term grows faster than the exponential term decays. One way to remedy this is to increase the

dissipation linearly with the *linear* system size: $\kappa = \kappa_0 L$. Then the thermodynamic limit is well-defined:

$$\lim_{L \to \infty} L \left(\frac{L!}{(L/2)!} \right) \left(\frac{\Delta}{\kappa_0 L} \right)^{L/2} = 0 \tag{191}$$

for $\Delta/\kappa_0 \ll 1$ such that the recovery to the eigenvalue goes to zero in the thermodynamic limit.

In conclusion, we have shown that the dissipative toric code with single-shot recovery jumps will host a qubit steady state structure in the presence of dephasing perturbations if the strength of the recovery process scales with the linear system size. Moreover, our analysis suggests that *any* local perturbation will not destroy the qubit steady state for such a system. As we discuss in the main text, the perturbative analysis also misses a non-perturbative contribution for the system's lifetime, which will result in a quantitatively different scaling dependence on Δ.

References

[1] B. M. Terhal, "Quantum error correction for quantum memories," *Rev. Mod. Phys.*, vol. 87, pp. 307–346, 2015.

[2] D. Gottesman, *Stabilizer codes and quantum error correction.* PhD thesis, California Institute of Technology, 1997.

[3] J. P. Paz and W. H. Zurek, "Continuous error correction," *Proc. R. Soc. A: Math. Phys. Eng. Sci.*, vol. 454, no. 1969, pp. 355–364, 1998.

[4] C. Ahn, A. C. Doherty, and A. J. Landahl, "Continuous quantum error correction via quantum feedback control," *Phys. Rev. A*, vol. 65, no. 4, p. 042301, 2002.

[5] M. Sarovar and G. J. Milburn, "Continuous quantum error correction by cooling," *Phys. Rev. A*, vol. 72, no. 1, p. 012306, 2005.

[6] H. Mabuchi, "Continuous quantum error correction as classical hybrid control," *New J. Phys.*, vol. 11, no. 10, p. 105044, 2009.

[7] O. Oreshkov, "Continuous-time quantum error correction," *arXiv:1311.2485*, 2013.

[8] V. V. Albert and P. Faist, eds., *The Error Correction Zoo.* 2023.

[9] Z. Leghtas, S. Touzard, I. M. Pop, A. Kou, B. Vlastakis, A. Petrenko, K. M. Sliwa, A. Narla, S. Shankar, M. J. Hatridge, M. Reagor, L. Frunzio, R. J. Schoelkopf, M. Mirrahimi, and M. H. Devoret, "Confining the state of light to a quantum manifold by engineered two-photon loss," *Science*, vol. 347, no. 6224, pp. 853–857, 2015.

[10] S. Touzard, A. Grimm, Z. Leghtas, S. O. Mundhada, P. Reinhold, C. Axline, M. Reagor, K. Chou, J. Blumoff, K. M. Sliwa, S. Shankar, L. Frunzio, R. J. Schoelkopf, M. Mirrahimi, and M. H. Devoret, "Coherent oscillations inside a quantum manifold stabilized by dissipation," *Phys. Rev. X*, vol. 8, p. 021005, 2018.

[11] J. M. Gertler, B. Baker, J. Li, S. Shirol, J. Koch, and C. Wang, "Protecting a bosonic qubit with autonomous quantum error correction," *Nature*, vol. 590, no. 7845, pp. 243–248, 2021.

[12] R. Lescanne, M. Villiers, T. Peronnin, A. Sarlette, M. Delbecq, B. Huard, T. Kontos, M. Mirrahimi, and Z. Leghtas, "Exponential suppression of bit-flips in a qubit encoded in an oscillator," *Nat. Phys.*, vol. 16, no. 5, pp. 509–513, 2020.

[13] B. de Neeve, T.-L. Nguyen, T. Behrle, and J. P. Home, "Error correction of a logical grid state qubit by dissipative pumping," *Nat. Phys.*, vol. 18, no. 3, pp. 296–300, 2022.

[14] P. Campagne-Ibarcq, A. Eickbusch, S. Touzard, E. Zalys-Geller, N. E. Frattini, V. V. Sivak, P. Reinhold, S. Puri, S. Shankar, R. J. Schoelkopf, L. Frunzio, M. Mirrahimi, and M. H. Devoret, "Quantum error correction of a qubit encoded in grid states of an oscillator," *Nature*, vol. 584, no. 7821, pp. 368–372, 2020.

[15] V. V. Sivak, A. Eickbusch, B. Royer, S. Singh, I. Tsioutsios, S. Ganjam, A. Miano, B. L. Brock, A. Z. Ding, L. Frunzio, S. M. Girvin, R. J. Schoelkopf, and M. H. Devoret, "Real-time quantum error correction beyond break-even," *Nature*, vol. 616, no. 7955, pp. 50–55, 2023.

[16] B. J. Brown, D. Loss, J. K. Pachos, C. N. Self, and J. R. Wootton, "Quantum memories at finite temperature," *Rev. Mod. Phys.*, vol. 88, p. 045005, 2016.

[17] R. Peierls, "On ising's model of ferromagnetism," *Math. Proc. Cambridge Philos. Soc.*, vol. 32, no. 3, p. 477–481, 1936.

[18] R. B. Griffiths, "Peierls proof of spontaneous magnetization in a two-dimensional ising ferromagnet," *Phys. Rev.*, vol. 136, pp. A437–A439, 1964.

[19] E. Dennis, A. Kitaev, A. Landahl, and J. Preskill, "Topological quantum memory," *J. Math. Phys.*, vol. 43, pp. 4452–4505, 2002.

[20] R. Alicki, M. Horodecki, P. Horodecki, and R. Horodecki, "On thermal stability of topological qubit in kitaev's 4d model," *Open Syst. Inf. Dyn.*, vol. 17, no. 01, pp. 1–20, 2010.

[21] F. Pastawski, L. Clemente, and J. I. Cirac, "Quantum memories based on engineered dissipation," *Phys. Rev. A*, vol. 83, p. 012304, 2011.

[22] Y.-J. Liu and S. Lieu, "Dissipative phase transitions and passive error correction," *arXiv:2307.09512*, 2023.

[23] S. Bravyi and B. Terhal, "A no-go theorem for a two-dimensional self-correcting quantum memory based on stabilizer codes," *New J. Phys.*, vol. 11, no. 4, p. 043029, 2009.

[24] O. Landon-Cardinal and D. Poulin, "Local topological order inhibits thermal stability in 2d," *Phys. Rev. Lett.*, vol. 110, p. 090502, 2013.

[25] J. Haah and J. Preskill, "Logical-operator tradeoff for local quantum codes," *Phys. Rev. A*, vol. 86, p. 032308, 2012.

[26] M. B. Hastings, "Topological order at nonzero temperature," *Phys. Rev. Lett.*, vol. 107, p. 210501, 2011.

[27] B. Yoshida, "Feasibility of self-correcting quantum memory and thermal stability of topological order," *Ann. Phys.*, vol. 326, no. 10, pp. 2566–2633, 2011.

[28] J. Haah, "Commuting pauli hamiltonians as maps between free modules," *Comm. Math. Phys.*, vol. 324, no. 2, pp. 351–399, 2013.

[29] F. Pastawski and B. Yoshida, "Fault-tolerant logical gates in quantum error-correcting codes," *Phys. Rev. A*, vol. 91, p. 012305, 2015.

[30] S. Hallgren, D. Nagaj, and S. Narayanaswami, "The local hamiltonian problem on a line with eight states is qma-complete," *Quantum Info. Comput.*, vol. 13, no. 9–10, p. 721–750, 2013.

[31] D. Aharonov, D. Gottesman, S. Irani, and J. Kempe, "The power of quantum systems on a line," *Comm. Math. Phys.*, vol. 287, pp. 41–65, 4 2009.

[32] N. Schuch, M. M. Wolf, F. Verstraete, and J. I. Cirac, "Computational complexity of projected entangled pair states," *Phys. Rev. Lett.*, vol. 98, p. 140506, 2007.

[33] S. Piddock and A. Montanaro, "The complexity of antiferromagnetic interactions and 2d lattices," *Quantum Info. Comput.*, vol. 17, no. 7–8, p. 636–672, 2017.

[34] J. Haah, "Local stabilizer codes in three dimensions without string logical operators," *Phys. Rev. A*, vol. 83, no. 4, p. 042330, 2011.

[35] A. Hamma, C. Castelnovo, and C. Chamon, "Toric-boson model: Toward a topological quantum memory at finite temperature," *Phys. Rev. B*, vol. 79, p. 245122, 2009.

[36] J. R. Wootton, "Topological phases and self-correcting memories in interacting anyon systems," *Phys. Rev. A*, vol. 88, p. 062312, 2013.

[37] S. Chesi, B. Röthlisberger, and D. Loss, "Self-correcting quantum memory in a thermal environment," *Phys. Rev. A*, vol. 82, p. 022305, 2010.

[38] E. Kapit, J. T. Chalker, and S. H. Simon, "Passive correction of quantum logical errors in a driven, dissipative system: A blueprint for an analog quantum code fabric," *Phys. Rev. A*, vol. 91, p. 062324, 2015.

[39] S. Lieu, Y.-J. Liu, and A. V. Gorshkov, "Candidate for a passively-protected quantum memory in two dimensions," *arXiv:2205.09767*, 2022.

[40] D. Gottesman, "Fault-Tolerant Quantum Computation with Constant Overhead," *arXiv:1310.2984*, 2013.

[41] T.-C. Lin and M.-H. Hsieh, "Good quantum ldpc codes with linear time decoder from lossless expanders," *arXiv:2203.03581*, 2022.

[42] A. Leverrier and G. Zémor, "Quantum tanner codes," in *2022 IEEE 63rd Annual Symposium on Foundations of Computer Science (FOCS)*, pp. 872–883, IEEE, 2022.

[43] P. Panteleev and G. Kalachev, "Asymptotically good quantum and locally testable classical ldpc codes," in *Proceedings of the 54th Annual ACM SIGACT Symposium on Theory of Computing*, pp. 375–388, 2022.

[44] R. Alicki, M. Fannes, and M. Horodecki, "On thermalization in kitaev's 2d model," *J. Phys. A: Math. Theor.*, vol. 42, no. 6, p. 065303, 2009.

[45] A. Lucia, D. Pérez-García, and A. Pérez-Hernández, "Thermalization in kitaev's quantum double models via tensor network techniques," *arXiv:2107.01628*, 2023.

[46] I. Bardet, A. Capel, L. Gao, A. Lucia, D. Pérez-García, and C. Rouzé, "Rapid thermalization of spin chain commuting hamiltonians," *Phys. Rev. Lett.*, vol. 130, p. 060401, 2023.

[47] H.-P. Breuer, F. Petruccione, *et al.*, *The theory of open quantum systems*. Oxford University Press on Demand, 2002.

[48] V. Gorini, A. Kossakowski, and E. C. G. Sudarshan, "Completely positive dynamical semigroups of n-level systems," *J. Math. Phys.*, vol. 17, no. 5, pp. 821–825, 1976.

[49] G. Lindblad, "On the generators of quantum dynamical semigroups," *Comm. Math. Phys.*, vol. 48, no. 2, pp. 119–130, 1976.

[50] E. Knill and R. Laflamme, "Theory of quantum error-correcting codes," *Phys. Rev. A*, vol. 55, pp. 900–911, 1997.

[51] A. L. Grimsmo, J. Combes, and B. Q. Baragiola, "Quantum computing with rotation-symmetric bosonic codes," *Phys. Rev. X*, vol. 10, p. 011058, 2020.

[52] V. V. Albert, B. Bradlyn, M. Fraas, and L. Jiang, "Geometry and response of lindbladians," *Phys. Rev. X*, vol. 6, p. 041031, 2016.

[53] V. V. Albert, "Lindbladians with multiple steady states: theory and applications," *arXiv:1802.00010*, 2018.

[54] *"NIST Digital Library of Mathematical Functions."* https://dlmf.nist.gov/, Release 1.1.9 of 2023-03-15. F. W. J. Olver, A. B. Olde Daalhuis, D. W. Lozier, B. I. Schneider, R. F. Boisvert, C. W. Clark, B. R. Miller, B. V. Saunders, H. S. Cohl, and M. A. McClain, eds.

[55] A. Kossakowski, "On quantum statistical mechanics of non-hamiltonian systems," *Rep. Math. Phys.*, vol. 3, no. 4, pp. 247–274, 1972.

[56] D. Gottesman, "Fault-tolerant quantum computation with higher-dimensional systems," *Chaos Solit. Fractals*, vol. 10, no. 10, pp. 1749–1758, 1999.

[57] J. Bierbrauer and Y. Edel, "Quantum twisted codes," *J. Comb. Des.*, vol. 8, no. 3, pp. 174–188, 2000.

[58] A. Ketkar, A. Klappenecker, S. Kumar, and P. K. Sarvepalli, "Nonbinary stabilizer codes over finite fields," *IEEE transactions on information theory*, vol. 52, no. 11, pp. 4892–4914, 2006.

[59] T. Cormen, C. Leiserson, R. Rivest, and C. Stein, *Introduction To Algorithms*. Mit Electrical Engineering and Computer Science, MIT Press, 2001.

[60] A. Kitaev, "Anyons in an exactly solved model and beyond," *Ann. Phys.*, vol. 321, no. 1, pp. 2–111, 2006.

[61] T. M. Stace, S. D. Barrett, and A. C. Doherty, "Thresholds for topological codes in the presence of loss," *Phys. Rev. Lett.*, vol. 102, p. 200501, 2009.

[62] D. K. Tuckett, A. S. Darmawan, C. T. Chubb, S. Bravyi, S. D. Bartlett, and S. T. Flammia, "Tailoring surface codes for highly biased noise," *Phys. Rev. X*, vol. 9, p. 041031, 2019.

[63] A. R. Calderbank, E. M. Rains, P. W. Shor, and N. J. A. Sloane, "Quantum error correction and orthogonal geometry," *Phys. Rev. Lett.*, vol. 78, pp. 405–408, 1997.

[64] C. Wang, J. Harrington, and J. Preskill, "Confinement-higgs transition in a disordered gauge theory and the accuracy threshold for quantum memory," *Ann. Phys.*, vol. 303, no. 1, pp. 31–58, 2003.

[65] J. Dengis, R. König, and F. Pastawski, "An optimal dissipative encoder for the toric code," *New J. Phys.*, vol. 16, no. 1, p. 013023, 2014.

[66] F. Ticozzi, G. Baggio, and L. Viola, "Quantum Information Encoding from Stabilizing Dynamics," in *2019 IEEE 58th Conference on Decision and Control (CDC)*, pp. 413–418, IEEE, 2019.

[67] M. H. Michael, M. Silveri, R. T. Brierley, V. V. Albert, J. Salmilehto, L. Jiang, and S. M. Girvin, "New class of quantum error-correcting codes for a bosonic mode," *Phys. Rev. X*, vol. 6, p. 031006, 2016.

[68] A. Kubica and J. Preskill, "Cellular-automaton decoders with provable thresholds for topological codes," *Phys. Rev. Lett.*, vol. 123, p. 020501, 2019.

[69] M. A. Nielsen and I. L. Chuang, *Quantum computation and quantum information*. Cambridge University Press, 10th anniversary ed ed.

[70] B. Buča and T. Prosen, "A note on symmetry reductions of the lindblad equation: transport in constrained open spin chains," *New J. Phys.*, vol. 14, no. 7, p. 073007, 2012.